

Tadpoles and Closed String Backgrounds in Open String Field Theory

Ian Ellwood, Jessie Shelton and Washington Taylor

Center for Theoretical Physics

MIT, Bldg. 6-308

Cambridge, MA 02139, U.S.A.

`iellwood@mit.edu, jshelton@mit.edu, wati@mit.edu`

ABSTRACT: We investigate the quantum structure of Witten's cubic open bosonic string field theory by computing the one-loop contribution to the open string tadpole using both oscillator and conformal field theory methods. We find divergences and a breakdown of BRST invariance in the tadpole diagram arising from tachyonic and massless closed string states, and we discuss ways of treating these problems. For a Dp -brane with sufficiently many transverse dimensions, the tadpole can be rendered finite by analytically continuing the closed string tachyon by hand; this diagram then naturally incorporates the (linearized) shift of the closed string background due to the presence of the brane. We observe that divergences at higher loops will doom any straightforward attempt at analyzing general quantum effects in bosonic open string field theory on a Dp -brane of any dimension, but our analysis does not uncover any potential obstacles to the existence of a sensible quantum open string field theory in the supersymmetric case.

KEYWORDS: String Field Theory.

Contents

1. Introduction	2
2. Perturbation theory in open string field theory	5
3. Evaluation of the tadpole using conformal field theory	6
3.1 Mapping the Witten diagram to the cylinder	7
3.2 The $T \rightarrow 0$ limit	9
3.3 Interpretation of the divergences	16
3.4 Lower dimensional Dp -branes	17
4. Evaluation of the tadpole using oscillator methods	19
4.1 Oscillator description of the one-loop tadpole	20
4.2 Divergences in the tadpole	22
4.3 The matrices M and R	25
4.4 Summary of oscillator calculation	27
5. The open string tadpole in open-closed string field theory	28
6. Divergences and closed strings	32
6.1 The leading divergence and the closed string tachyon	32
6.2 Tadpole contributions from massless closed strings	33
6.3 Divergent diagrams and BRST invariance	34
6.4 Beyond one loop	38
7. Discussion	39
A. The BRST anomaly in the D25-brane theory	42
A.1 The BRST anomaly in the conformal field theory method	43
A.2 The BRST anomaly in level truncation	44
B. The infinite level limit	45

1. Introduction

String field theory is a space-time formulation of string theory which may have the capacity to describe all string backgrounds in terms of a common set of degrees of freedom. Much recent interest in Witten's open string field theory (OSFT) [1] has been centered around the discovery that this theory can describe D-branes as classical solitons, so that distinct open string backgrounds not related through marginal deformations can appear as solutions of a single set of equations of motion (for reviews see [2, 3, 4, 5, 6]). Most of the recent work in this area has focused on classical aspects of OSFT (although, for some recent papers which address quantum features of the theory, see [7]).

In order for string field theory to have a real chance at addressing any of the deep unsolved problems in string theory/quantum gravity, it is clearly necessary that the theory should be well defined quantum mechanically. In an earlier phase of work, some progress was made in understanding the quantum structure of OSFT. This work is summarized and described in the language of BV quantization by Thorn in his review [8]. In this paper we extend this earlier work by carrying out a systematic analysis of the one-loop open string tadpole diagram in Witten's bosonic OSFT. We analyze the divergence structure of this diagram and the role which closed strings play in the structure of the tadpole, and we describe the implications of this analysis for the quantum theory.

An important aspect of quantum open string field theory is the role which closed strings play in the theory. As has been known since their first discovery [9, 10], closed strings appear as poles in nonplanar one-loop amplitudes of open strings. An analysis of these poles in the one-loop nonplanar two-point function of OSFT was given in [11]. Because of the existence of these intermediate closed string states, any unitary quantum open string field theory must include some class of composite asymptotic states which can be identified with closed strings. These asymptotic states have not yet been explicitly identified in OSFT, although related open string states which can be used to compute amplitudes including closed strings in OSFT are described in [12, 13, 14, 15, 16, 17]; other approaches to understanding how closed strings appear in OSFT were pursued in [18]. In this paper, we consider the appearance of closed strings in OSFT from a different point of view than has been taken in previous work on the subject. We show that an important part of the structure of the open string tadpole comes from the closed string tadpole, which in the presence of a D-brane describes the linearized gravitational fields of that D-brane. This demonstrates that not only do the closed strings appear as poles in the open string theory, but that they also take expectation values in response to D-brane sources within the context of OSFT; this provides a new perspective on the role of closed strings in OSFT.

The relationship between open and closed strings is central to the concept of holography and the AdS/CFT correspondence [19, 20, 21]. In the AdS/CFT correspondence, a decoupling limit is taken where open strings on a brane are described by a conformal field theory; this theory has a dual description as a near-horizon limit of the closed string (gravity) theory

around the D-brane. A complete quantum open string field theory would generalize this picture; if OSFT can be shown to be unitary without explicitly including the closed strings as additional dynamical degrees of freedom, we would have a more general holographic theory in which the open string field theory on a D-brane would encode the gravitational physics in the full D-brane geometry in a precise fashion. While we do not directly address these ideas in this paper, some further discussion in this direction is included at the end of the paper.

Until recently, only a few diagrams had been explicitly evaluated in OSFT: the Veneziano amplitude [22, 23, 24], and the non-planar two-point function [11]. These diagrams were computed by explicitly mapping the Witten parameterization of string field theory to a parameterization more natural for conformal field theory, and then computing the diagram explicitly in CFT. There has recently been some renewed interest in studying perturbative aspects of OSFT by developing new techniques for calculating diagrams in the theory [25, 31]. Using these methods it is possible to compute any OSFT diagram to a high degree of accuracy using the level truncation method on oscillators. This method provides an alternative to the CFT method, and gives some information about a wider range of diagrams while lacking the analytic control of the CFT method. In this paper we use both methods, finding that each gives useful information.

The one-loop tadpole diagram we consider in this paper is perhaps the simplest of the one-loop diagrams in OSFT. While a preliminary study of this diagram was done in [8, 25], we expand on the analysis presented in [25] and augment it by using the conformal field theory method to give an alternate expression for the diagram. We also generalize the discussion by computing the diagram for OSFT defined on a Dp -brane background for any p .

The one-loop tadpole diagram has divergences of several kinds. As the modular parameter T describing the length of the internal open string propagator becomes large, there is a divergence from the open string tachyon. This divergence is easy to understand, and can be removed by analytic continuation in the oscillator approach to OSFT. In addition to the large T divergence of the diagram, there are divergences as $T \rightarrow 0$. In the conformal frame natural to OSFT this limit corresponds to a pinching off of the world-sheet. In an alternate conformal frame, however, the small open string loop gives rise to a long closed string tube. These two conformal frames are displayed in figure 1. Since the propagation

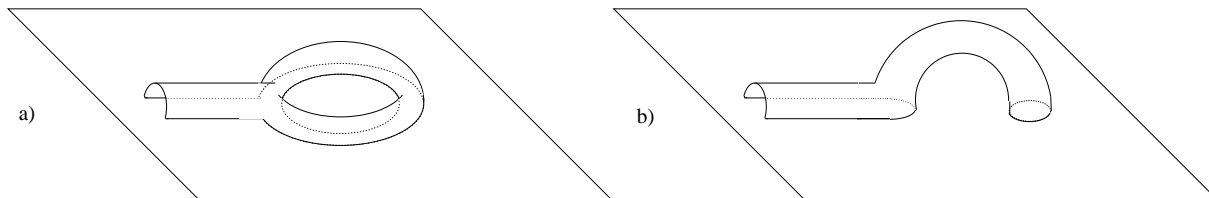


Figure 1: Two conformally equivalent pictures of the one-loop open string tadpole. a) The open string tadpole is represented as a purely open string process in which a single open string splits into two open strings which then collide. b) The open string tadpole is represented as a transition between an open string and a closed string. The closed string is absorbed into the brane.

over long distances of massive fields is suppressed, only the tachyon and the massless sector of the closed strings contribute to the $T \rightarrow 0$ divergences of the tadpole. Using both the conformal field theory and oscillator approaches, we isolate the $T \rightarrow 0$ divergences in the one-loop tadpole diagram. By extracting the leading divergences of the tadpole, we can separate the divergence arising from the tachyon from any divergences associated with the graviton/dilaton in the massless sector.

The divergence from the closed string tachyon arises because of the usual problem that the Euclidean theory has a real exponent in the Schwinger parameterization of the propagator, and diverges for tachyonic modes. This problem is usually dealt with by a simple analytic continuation. In this case, however, the analytic continuation is rather subtle, as the closed string degrees of freedom which are causing the divergence are not fundamental degrees of freedom in the theory. In the one-loop diagram we study in this paper, the analytic continuation can be done by hand in the CFT approach by explicitly using our understanding of the closed string physics underlying the divergence. Even for this relatively simple diagram, however, there are a number of subtleties in this analytic continuation, and to ensure that we completely remove all the tachyonic divergences we are forced to consider lower-dimensional brane backgrounds. In a more general context, such as for higher-loop diagrams, it would be difficult to systematically treat this type of divergence using open string field theory.

Assuming that the divergence from the closed string tachyon is dealt with by a form of analytic continuation, we are left with possible divergences from the massless closed string states. Such divergences appear only when considering the open string theory on a Dp -brane with $p \geq 23$. This is essentially because the open string tadpole is generated directly from the closed string tadpole, and the closed string tadpole arises from the solution of the linearized gravitational equations with a Dp -brane source [26, 27]. Since a brane of codimension 2 has a long-range potential which goes as $\ln r$, while a brane of codimension 3 has a potential going as $1/r$, we need at least three codimensions to remove the divergences from the massless sector. In general, whether the tadpole is finite or divergent, we find that the structure of the linearized closed string fields in the D-brane background is encoded in the open string tadpole.

After analyzing the divergence structure of the one-loop tadpole, we also consider briefly what one might expect of OSFT at two or more loops. We consider in particular the two loop non-planar diagram which represents a torus with a hole in it. This diagram contains as a subdiagram the closed string one point function which suffers from a BRST anomaly [28, 29, 30, 26] in world-sheet perturbation theory. We conjecture that in OSFT this diagram will lead to a divergence and BRST anomaly. Since this divergence is purely closed-string in nature, it should occur for the theory on a Dp -brane for any p , and poses a serious problem for any attempt to make sense of the bosonic open string field theory as a complete quantum theory.

In Section 3 we compute the one-loop tadpole using conformal field theory methods. In section 4 we compute the same diagram using oscillator methods. Section 5 contains a discussion of the one-loop open string tadpole in Zwiebach's open-closed string field theory, where the structure of the diagram is somewhat more transparent. Section 6 synthesizes the results of the preceding sections, and contains a general discussion of the divergences of the tadpole and the role of closed strings in the tadpole. Section 7 contains some concluding remarks. In two appendices we include some technical points. Appendix A contains a discussion of the BRST anomaly in the D25-brane theory. Appendix B contains some comments on the infinite-level limit of the level truncation method used in Section 4.

2. Perturbation theory in open string field theory

We begin with a summary of Witten's formulation of open bosonic string field theory (OSFT) [1] with an emphasis on perturbation theory. For general reviews of OSFT see [32, 33, 8, 5]. The classical field for OSFT is a ghost number one state, Ψ , in the free open string Fock space. The string field, Ψ , has a natural expansion in terms of the open string fields

$$\Psi = \int d^{26}p [\phi(p)c_1|0;p\rangle + A_\mu(p)\alpha_{-1}^\mu c_1|0;p\rangle + \psi(p)c_0|0;p\rangle + \dots], \quad (2.1)$$

where ϕ is the open string tachyon, A_μ is the gauge field and ψ is an auxiliary field. The vacuum $|0\rangle$ denotes the $SL(2, \mathbf{R})$ vacuum. The classical action is given by

$$S(\Psi) = \frac{1}{2} \int \Psi \star Q_B \Psi + \frac{g}{3} \int \Psi \star \Psi \star \Psi. \quad (2.2)$$

The definitions for the \star -product and string integration are given in [32, 34, 35, 36, 37, 38, 39] in terms of both oscillator expressions and conformal field theory correlators. We will also make use of two-string and three-string vertices, $\langle V_2|$ and $\langle V_3|$, which are defined by

$$\langle V_2||\Psi_1\rangle|\Psi_2\rangle = \int \Psi_1 \star \Psi_2, \quad (2.3)$$

$$\langle V_3||\Psi_1\rangle|\Psi_2\rangle|\Psi_3\rangle = \int \Psi_1 \star \Psi_2 \star \Psi_3, \quad (2.4)$$

and are elements of the two-string and three-string Fock spaces respectively.

The theory has a large gauge group. Infinitesimally the gauge transformations are given by

$$\Psi \rightarrow \Psi + Q_B \Lambda + g(\Psi \star \Lambda - \Lambda \star \Psi), \quad (2.5)$$

where Λ is any ghost number 0 field.

To quantize the theory we must fix a gauge. The standard choice for gauge fixing is Feynman-Siegel (FS) gauge fixing which imposes the condition $b_0\Psi = 0$. It is straightforward to perform tree-level calculations in this gauge, but some care is required when trying to

impose this condition on path integrals. Roughly speaking, it turns out that if one tries to introduce Fadeev-Popov ghosts to fix $b_0\Psi = 0$, the ghosts themselves suffer from a gauge redundancy similar to the gauge redundancy of the original action. To fix this new gauge redundancy one must introduce ghosts for ghosts. As the new ghosts have their own redundancy, this process proceeds forever, creating an infinite tower of ghost fields. Happily, at the end of the day this entire procedure can be summarized as follows [8]:

1. The field Ψ is fixed by $b_0\Psi = 0$.
2. The ghost number of Ψ is allowed to range over all ghost numbers, not just ghost number 1. The fields of ghost numbers other than one are all ghost fields.
3. Ψ is a grassmann odd field. To define what this means, suppose the states $\{|s\rangle\}$ form a basis for the open string Fock space such that each $|s\rangle$ has definite ghost number. Then if we write Ψ in a Fock space expansion as $\Psi = \sum_s |s\rangle\psi_s$, then ψ_s has the opposite grassmannality of $|s\rangle$.

The form of the action remains the same as in equation (2.2). Using the FS gauge condition of Ψ we can simplify the kinetic term:

$$S_{FS}(\Psi) = \frac{1}{2} \int \Psi \star c_0 L_0 \Psi + \frac{g}{3} \int \Psi \star \Psi \star \Psi. \quad (2.6)$$

Given the gauge fixed action we can now develop the Feynman rules for perturbation theory. We can do this in two ways, which we will refer to as the conformal field theory method and the oscillator method.

In the conformal field theory method, the Feynman rules are given in terms of rules for sewing strips of world-sheet together. Amplitudes may be evaluated by conformally mapping the resulting diagrams to the upper half plane for genus 0 or the cylinder for genus 1.

In the oscillator method the Feynman rules are calculated directly from the action using the usual methods from field theory but summing over the infinite number of fields. For any amplitude this gives rise to correlators which can be evaluated using squeezed state methods.

In the next two sections we consider each of these two methods in turn.

3. Evaluation of the tadpole using conformal field theory

In this section we calculate the one-point function using conformal field theory methods. We begin the calculation with the assumption that we are working with the theory on a D25-brane. In section 3.1 we describe how the diagram can be computed by constructing a map from the original Witten diagram to the cylinder. In section 3.2, we specialize to the limit where the internal loop of the diagram is small and study the divergences in this limit. In section 3.3 we discuss the origin of these divergences from the propagation of closed string

modes over long distances (these divergences are discussed further in Section 6). Finally, in section 3.4 we discuss how the calculation differs for the theory on a Dp -brane with $p \neq 25$.

3.1 Mapping the Witten diagram to the cylinder

We begin with a brief discussion of the world-sheet interpretation of FS gauge fixed OSFT. The derivation of this interpretation is given in [40, 41, 8, 42]. The Feynman rules consist of one propagator and one vertex.

The propagator is given by an integral over world-sheet strips of fixed width. By convention the strips are of width π , and length T , where T is integrated from 0 to ∞ . To ensure the right measure on moduli space $b(\sigma)$ is integrated across the strip [40].

The only vertex in the theory is a prescription for gluing three strips together. The right half of the first strip is glued to the left half of the second and similarly for the second and third strips and the third and first strips.

Using these rules we can construct the one-point amplitude. We start with an external state $|A\rangle$ which propagates along a strip of length T_A . We then take a second strip of length T and glue both ends of it and the end of the first propagator together using the vertex. The resulting diagram is pictured in figure 2.

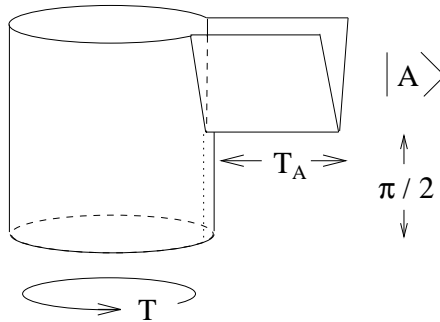


Figure 2: The world-sheet diagram for the one-point function.

We wish to study this diagram using conformal field theory methods. To do this we use the methods of [11] to map the diagram to a cylinder. For another approach to this conformal mapping problem, see [43]. Taking the limit $T_A \rightarrow \infty$, we can map the external state, $|A\rangle$, to a puncture at the boundary of the cylinder.

It is convenient to flatten the diagram by cutting along the folded edge of the external propagator in figure 2 and cutting the internal propagator in half. The resulting diagram is displayed in figure 3 a. We will let ρ be the coordinate on the Witten diagram and u be the coordinate on the cylinder. To enforce Neumann boundary conditions along the boundaries of the diagram, we use the doubling trick. Since the double of the cylinder is a torus, we may use the theory of elliptic functions to determine $\rho(u)$.

Consider the image of the Witten diagram under $\rho \rightarrow u$ shown in figure 3 b. The top and bottom of the diagram are identified as well as the left and right edges. The external state, $|A\rangle$, is mapped to a puncture at point A which we choose to be at $u = 0$. The midpoint is mapped to point β . By the symmetry in the diagram, we can set the real part of β to zero. Since the vertex in the original Witten diagram had an angle of 3π , the function $\rho(u)$ must behave as $\rho(u) - \rho(\beta) \sim (u - \beta)^{3/2}$ near β . This implies that $d\rho/du$ has a branch cut. The height of the torus is given by a purely imaginary parameter τ to be determined later.

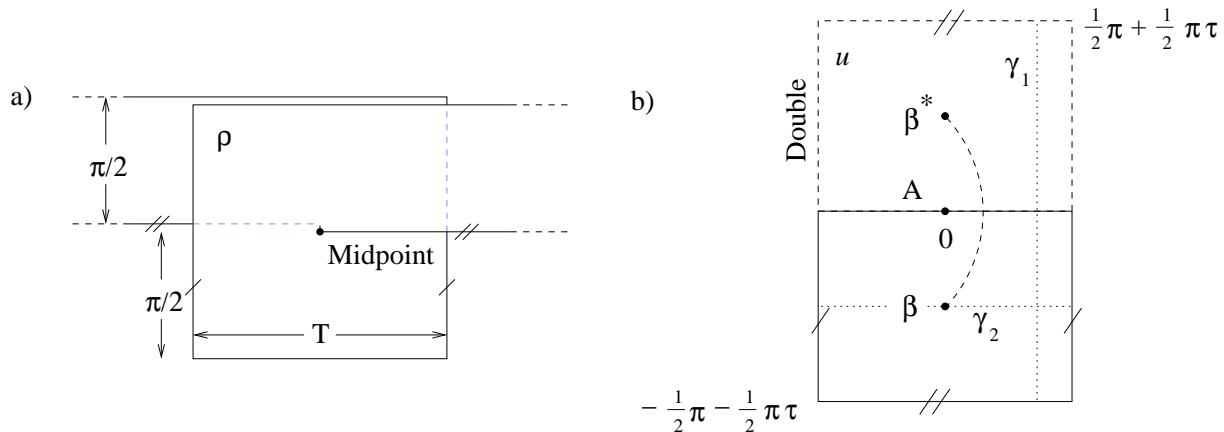


Figure 3: a) The tadpole diagram laid flat by cutting the external propagator along its middle and cutting the internal propagator in half. The edges to be identified are indicated by dashes. b) The doubled image of the tadpole under the conformal map $u(\rho)$. The left and right sides of the image are identified as well as the top and bottom. The image of the midpoint of the vertex is denoted by β .

The integral around the puncture A of $d\rho/du$ corresponds¹, in the original Witten diagram, to the total width of the external propagator plus its double, which is fixed to be $2\pi i$. This implies that $d\rho/du$ has a simple pole at A of residue one.

We now define the quadratic differential $\phi(u) = (\frac{d\rho}{du})^2(u)$. From the form of $d\rho/du$ near β we see that $\phi(u)$ has no branch cut, just a simple zero at β . In order to preserve Neumann boundary conditions we must also include a zero at the image of β under the doubling. Since we have put the top of the diagram along the real axis, we just get a second zero at β^* . The only other piece of analytic structure we need is that since $d\rho/du$ had a simple pole at A , $\phi(u)$ has a double pole at A .

Now since $\phi(u)$ is a meromorphic function on a torus we may determine it using ϑ -functions:

$$\phi(u) = C \frac{\vartheta_1(u - \beta, q)\vartheta_1(u - \beta^*, q)}{\vartheta_1^2(u, q)}, \quad (3.1)$$

where $q = e^{i\pi\tau}$. The constant C is determined from the condition that $\sqrt{\phi(u)}$ has a pole of residue one at A :

$$C = \frac{(\vartheta_1'(0))^2}{\vartheta_1(-\beta)\vartheta_1(-\beta^*)}. \quad (3.2)$$

The two constants β and τ can be determined from the height and width of the diagram by integrating $d\rho/du$ along the curves γ_1 and γ_2 . We have

$$\begin{aligned} \oint_{\gamma_1} du \sqrt{\phi(u)} &= 2\pi i, \\ \oint_{\gamma_2} du \sqrt{\phi(u)} &= T. \end{aligned} \quad (3.3)$$

¹One has to be careful that the contour does not cross the branch cut so that, in the ρ coordinates, the contour is continuous.

In general these relations cannot be solved analytically, but it is straightforward to solve them numerically and thus to determine τ and β as functions of T .

At this point one could, in principle, evaluate the diagram for any given A . If we suppose that the state A is defined by a vertex operator inserted on a half-disk with coordinates v , we can easily compute the map $\rho(v)$ from the half-disk to the tadpole diagram. The diagram at a fixed modular parameter is then computed by evaluating

$$\langle (u(\rho) \circ \rho(v) \circ A)(u(\rho) \circ \frac{1}{2\pi i} \int d\rho b(\rho)) \rangle_{\text{torus}} \quad (3.4)$$

where the contour of integration runs across the internal propagator. This correlator implicitly defines a fock space state, $|\mathcal{T}(T)\rangle$, given by

$$\langle A|\mathcal{T}(T)\rangle \equiv \langle (u(\rho) \circ \rho(v) \circ A)(u(\rho) \circ \frac{1}{2\pi i} \int d\rho b(\rho)) \rangle_{\text{torus}}. \quad (3.5)$$

Note that the state $|\mathcal{T}(T)\rangle$ is a function of the modular parameter T . The full tadpole diagram is given by integrating over this modular parameter. We thus define the full tadpole state $|\mathcal{T}\rangle$ by

$$|\mathcal{T}\rangle = \int_0^\infty dT |\mathcal{T}(T)\rangle. \quad (3.6)$$

The expression (3.4) can only be evaluated numerically, since we do not know $\rho(u)$ explicitly (only its derivative) and we cannot analytically solve the constraints (3.3). Furthermore, there are several types of divergences in the integral over T in (3.6). The integrand (3.5) diverges as $T \rightarrow \infty$ due to the open string tachyon. While this divergence is difficult to treat in the CFT approach, its physical origin is clear and is quite transparent in the oscillator approach, where this divergence can be treated by a suitable analytic continuation. We discuss the open string tachyon divergence further in Sections 4 and 6. In addition to the the divergence as $T \rightarrow \infty$, there are further divergences as $T \rightarrow 0$ arising from the closed string. These divergences are much more subtle, as closed strings are not explicitly included among the degrees of freedom in OSFT, but arise as composite states of highly excited open strings. We thus seek to evaluate the tadpole diagram in an expansion around $T = 0$, where much of the interesting physics in the diagram is hidden.

3.2 The $T \rightarrow 0$ limit

We now focus on the region of moduli space near $T = 0$. Unfortunately the map $\sqrt{\phi(u)}$ cannot easily be expanded around this limit. To get around this we use a trick. It turns out that the conformal map greatly simplifies if, instead of fixing the integral along γ_1 to be $2\pi i$, we set it equal to some parameter H and take $H \rightarrow i\infty$ holding T fixed. This is equivalent to gluing a semi-infinite cylinder to the bottom of the tadpole. Later we will see how to replace this long cylinder with a boundary state to reduce back to the finite length cylinder case, but for the moment we just consider the conformal map in this limit.

By solving the constraints (3.3) numerically, one can verify that as $H \rightarrow \infty$ with T fixed, β limits to a constant β_0 , while $\tau \rightarrow i\infty$. Recalling that $q = e^{i\pi\tau}$, we see that since τ is pure imaginary, $q \rightarrow 0$ as $H \rightarrow \infty$. Thus we may set $q = 0$ in our map to get

$$\left. \frac{d\rho}{du} \right|_{q=0} = \left. \sqrt{\phi(u)} \right|_{q=0} = \sqrt{\cot^2(u) - \cot^2(\beta_0)}. \quad (3.7)$$

We can now solve for T in terms of β_0 by performing the integral along γ_2 :

$$T = \oint_{\gamma_2} du \sqrt{\cot^2(u) - \cot^2(\beta_0)} = -\frac{i\pi}{\sin(\beta_0)}. \quad (3.8)$$

Using this relation, we can eliminate β_0 from the definition of our conformal map:

$$\lim_{H \rightarrow \infty} \left(\frac{d\rho}{du} \right) = \sqrt{1 + \left(\frac{T}{\pi} \right)^2 + \cot^2(u)}. \quad (3.9)$$

This function may even be integrated analytically although the resulting expression is cumbersome. For notational simplicity we now consider $d\rho/du$ only in the limit of $H \rightarrow \infty$ and we will assume that the tadpole diagram has an infinitely long tube extending from the bottom.

Before we consider the effect of replacing the long tube at the bottom of the diagram with a boundary state, we consider the effect of the map $\rho(u)$ on the external state A as $T \rightarrow 0$. Note that if we take the limit that $T \rightarrow 0$, $d\rho/du$ simplifies even further.

$$\lim_{T \rightarrow 0} \left(\frac{d\rho}{du} \right) = \sqrt{1 + \cot^2(u)} = \frac{1}{\sin(u)}, \quad (3.10)$$

where one must be careful about the interpretation of the branch cuts. Integrating this function yields

$$\int du \frac{1}{\sin(u)} = \log \left(-\tan \left(\frac{u}{2} \right) \right). \quad (3.11)$$

While this may not seem like a familiar map, it is actually a representation of the identity state. Putting

$$h(z) = \frac{1 + iz}{1 - iz}, \quad (3.12)$$

we consider the circle of conformal maps pictured in figure 4. One can verify that traversing the diagram counterclockwise (starting from the vertical strip at the bottom and proceeding to the representation of the identity in the upper left), gives the same map as $\rho(u)$ when $T \rightarrow 0$. This implies that the tadpole diagram with a long tube attached to the bottom is conformally equivalent to the identity state with an operator inserted in the corner in the limit $T \rightarrow 0$. Such states are known as Shapiro-Thorn states [12, 13].

We now must deal with the fact that the original diagram had a tube of finite length extending from the bottom. We thus consider the effect of replacing the infinite tube at

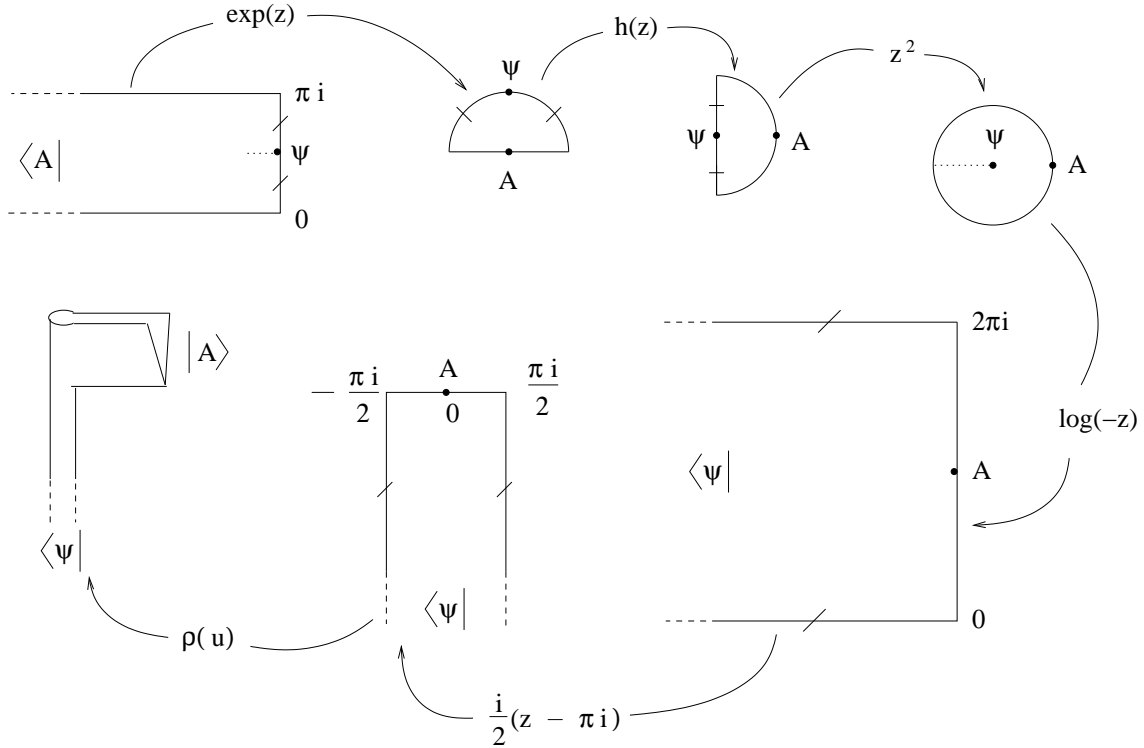


Figure 4: A circle of conformal maps showing the equivalence of the two prescriptions for the identity state. In the limit that $T \rightarrow 0$ traversing the diagram clockwise from the surface in the upper left to the tadpole in the bottom left is equivalent to the trivial map $f(z) = z$.

the bottom of the tadpole with the closed string boundary state with Neumann boundary conditions. The boundary state in disk coordinates for Neumann boundary conditions can be written

$$\langle \mathcal{B} | = \langle 0 | (\tilde{c}_{-1} + c_1)(\tilde{c}_0 + c_0)(\tilde{c}_1 + c_{-1}) \exp \left(\sum_{m>1} b_m \tilde{c}_m + \tilde{b}_m c_m \right) \exp \left(\sum_{n \geq 1} \frac{1}{n} \alpha_n \cdot \tilde{\alpha}_n \right) \quad (3.13)$$

where the oscillators are the usual closed string oscillators and $\langle 0 |$ is the closed string $SL(2, \mathbf{R})$ vacuum. When we map to cylinder coordinates, the disk becomes a semi-infinite tube with the boundary state being propagated in from infinity. By rescaling the size of the cylinder we can make it the same circumference as the long tube at the bottom of the tadpole.

Consider taking the long tube that extends from the bottom of the diagram and cutting it off a distance $\pi/2$ below the vertex. We can then attach the boundary state, in cylinder coordinates, onto the bottom of the diagram. Before adding the boundary state, the topology of the tadpole diagram is an annulus with one vertex operator (representing the external state) inserted on the outer boundary. Attaching the boundary state plugs the hole in the annulus, changing the topology to a disk. The cost of doing this is that there is now an additional vertex operator, representing the boundary state, inserted in the interior of the disk. For

general values of the modulus T , the complexity of the boundary state makes this replacement impractical, but, for small T , only a few terms in the boundary state become relevant.

After this modification, we can map the tadpole diagram to the unit disk with the image of the boundary state at $z = 0$ and the image of the state $|A\rangle$ at $z = 1$, where z is the coordinate on the disk. We call the coordinates on the boundary state disk w . Since the boundary state is not conformally invariant, it will be mapped to $z(w) \circ \mathcal{B}$. As before, we denote by v the coordinates on the half-disk where the vertex operator for the external state A is defined and we let $z(v)$ be the map that takes the external state A into the disk coordinates. We can then write down a formal expression for the tadpole diagram

$$\langle (z(v) \circ A)(z(\rho) \circ \frac{1}{2\pi i} \int d\rho b(\rho))(z(w) \circ \mathcal{B}) \rangle_{\text{disk}}. \quad (3.14)$$

Mapping everything to the upper-half plane using the map $h(z)$ defined in (3.12), we can write this as an inner product between A and the ket $|\mathcal{T}(T)\rangle$ defined in (3.5). If $|A\rangle$ is the external state in half-disk coordinates, the diagram at fixed modular parameter is given by

$$\langle A | U_{h(z) \circ z(v)}^\dagger (h(z) \circ z(\rho) \circ \frac{1}{2\pi i} \int d\rho b(\rho)) (h(z) \circ z(w) \circ \mathcal{B}) | 0 \rangle \quad (3.15)$$

which implies that

$$|\mathcal{T}(T)\rangle = U_{h(z) \circ z(v)}^\dagger (h(z) \circ z(\rho) \circ \frac{1}{2\pi i} \int d\rho b(\rho)) (h(z) \circ z(w) \circ \mathcal{B}) | 0 \rangle, \quad (3.16)$$

where the operator U_f is defined by its action on local operators

$$U_f \mathcal{O} U_f^{-1} = f \circ \mathcal{O}. \quad (3.17)$$

and U_f^\dagger is the BPZ dual of U_f . Such operators have been considered in [44, 45, 46, 47].

Since, as we've already discussed, the map $z(v)$ just limits to a representation of the identity state as $T \rightarrow 0$, the operator $U_{h(z) \circ z(v)}^\dagger$ has a well behaved limit as $T \rightarrow 0$. Thus, when we analyze the small T limit, we only need to focus on the behavior of $z(w) \circ \mathcal{B}$ and $z(\rho) \circ \int d\rho b(\rho)$. As it turns out, it is computationally easier to calculate $w(z)$ rather than $z(w)$. Pictorially, $w(z)$ is given in figure 5.

The map from the disk to the vertical strip is given by

$$u(z) = \frac{i}{2} \log(z). \quad (3.18)$$

Since we already know the derivative of the map from the vertical strip to the Witten diagram, $d\rho/du$, we can easily compute the derivative of the map from the disk to the Witten diagram. To eliminate excess factors of π , we put $W = T/\pi$. We then have

$$\frac{d\rho}{dz} = \frac{d\rho}{du}(u(z)) \frac{du}{dz} = \frac{i}{2} \frac{\sqrt{W^2(z-1)^2 - 4z}}{z(z-1)}. \quad (3.19)$$

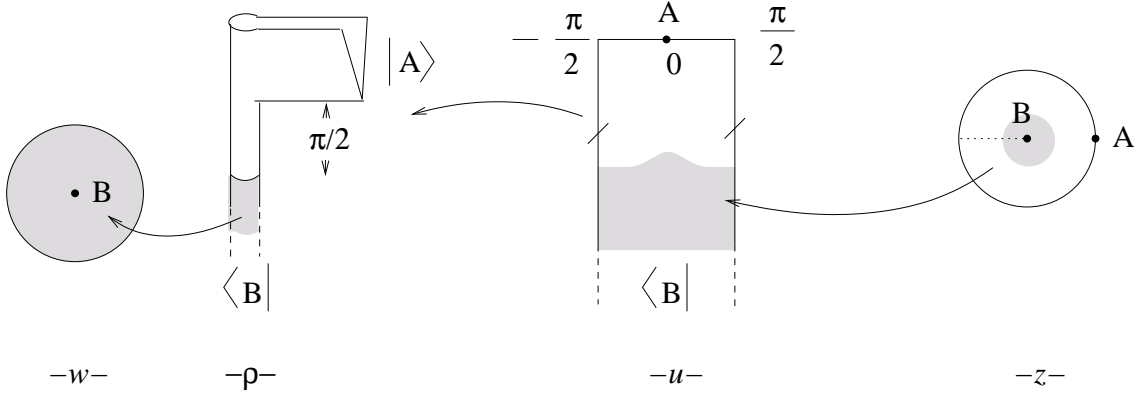


Figure 5: The map $w(z)$ is shown as a series of maps. The shaded regions show the images of the boundary state.

Integrating this function gives

$$\begin{aligned} \rho(z) = & -\frac{i}{2} \left(2 \tan^{-1} \left(\frac{1+z}{\sqrt{W^2(z-1)^2 - 4z}} \right) - W \log(z) \right. \\ & \left. + W \log(-2z + (1+z)W \sqrt{W^2(z-1)^2 - 4z} + W^2(1+z^2)) \right) + g(W), \end{aligned} \quad (3.20)$$

where $g(W)$ is the constant of integration. By fixing the image of the midpoint, we can determine $g(W)$ to be

$$g(W) = \frac{i}{2} \left(\pi + 2 \cot^{-1}(W) + i \log \left(\frac{W+i}{W-i} \right) + W \log(2 + 2W^2) \right). \quad (3.21)$$

Finally, we map the bottom of the Witten diagram to the disk with the boundary state in the center. This map is given by

$$w(\rho) = \exp \left(\frac{\pi - 2i\rho}{W} \right). \quad (3.22)$$

We can thus calculate $w(\rho(z)) = w(z)$. Since the full expression is quite complicated we only display the series expansion:

$$w(z) = e^{\pi/W + i \log(\frac{W+i}{W-i})/W} \left[-\frac{1+W^2}{W^2} z + 2 \frac{1+W^2}{W^4} z^2 + \frac{2W^4 + W^2 - 1}{W^6} z^3 + \mathcal{O}(z^4) \right]. \quad (3.23)$$

We can now find $z(w)$ as a power series in w . Putting

$$k(W) = e^{-\pi/W - i \log(\frac{W+i}{W-i})/W}, \quad (3.24)$$

we have

$$z(w) = -k \frac{W^2}{1+W^2} w + 2k^2 \frac{W^2}{(1+W^2)^2} w^2 - k^3 \frac{W^2(7+2W^2)}{(1+W^2)^3} w^3 + \mathcal{O}(w^4). \quad (3.25)$$

As one might expect, the unit disk is mapped to smaller and smaller regions as $W \rightarrow 0$. This suggests that the boundary state might be mapped to some local operator. In fact, all the positive weight parts of $|B\rangle$ will be suppressed in the small W limit. Thus the only relevant terms from the boundary state are the weight zero and weight $(-1, -1)$ fields. These are given by

$$\begin{aligned} |\mathcal{B}\rangle = & c_1(c_0 + \tilde{c}_0)\tilde{c}_1|0\rangle \\ & + \alpha_{-1} \cdot \tilde{\alpha}_{-1}c_1(c_0 + \tilde{c}_0)\tilde{c}_1|0\rangle - (c_1c_{-1} + \tilde{c}_{-1}\tilde{c}_1)(c_0 + \tilde{c}_0)|0\rangle \\ & + \text{higher weight states.} \end{aligned} \quad (3.26)$$

Since the term $c_1(c_0 + \tilde{c}_0)\tilde{c}_1|0\rangle$ is a weight $(-1, -1)$ primary it picks up the coefficient

$$\left(\frac{1+W^2}{kW^2}\right)^2 \quad (3.27)$$

under the $z(w)$ map. Similarly, the term $\alpha_{-1} \cdot \tilde{\alpha}_{-1}\tilde{c}_1(c_0 + \tilde{c}_0)c_1|0\rangle$ is a weight $(0, 0)$ primary and thus is unchanged by the $z(w)$ map.

Unfortunately, the term, $-(c_1c_{-1} + \tilde{c}_{-1}\tilde{c}_1)(c_0 + \tilde{c}_0)|0\rangle$, is not a primary and is mapped to

$$\begin{aligned} & -(c_1c_{-1} + \tilde{c}_{-1}\tilde{c}_1)(c_0 + \tilde{c}_0)|0\rangle - \frac{8}{W^4}c_1(c_0 + \tilde{c}_0)\tilde{c}_1|0\rangle \\ & + \frac{4}{W^2}c_1(c_{-1} + \tilde{c}_{-1})\tilde{c}_1|0\rangle + \frac{2}{W^2}(c_1 - \tilde{c}_1)c_0\tilde{c}_0. \end{aligned} \quad (3.28)$$

As can be seen in the second term, this state mixes with the weight $(-1, -1)$ state $c_1(c_0 + \tilde{c}_0)\tilde{c}_1|0\rangle$ under conformal maps. This mixing will play a role later.

To fully account for the behavior of the tadpole near $W \rightarrow 0$, we must take care of the insertion of the b_0 . Since the conformal map from the disk to the tadpole has already been found, the transformation of b_0 to the disk coordinates is straightforward. Calling the resulting operator B , we get

$$B = \frac{1}{\pi} \int dz \frac{z(z-1)}{\sqrt{W^2(z-1)^2 - 4z}} b(z) - \text{c.c.}, \quad (3.29)$$

where the contour runs along the real axis from -1 to $z(-1)$. Note that as $W \rightarrow 0$, $z(-1) \rightarrow 0$ also. Thus we can get collisions between $b(z)$ and the various c 's in the boundary state. We can expand B in terms of the modes found in equation (3.26), keeping only the most divergent terms for each mode b_n :

$$B \sim \dots - \frac{4}{3\pi} b_{-1} + \frac{1}{W^2} b_0 - \frac{1}{\pi W^3 k} b_1 + \dots - \text{c.c.} \quad (3.30)$$

We can now let B act on the conformally transformed boundary state. We keep only the most divergent terms from each state and drop all finite terms:

$$\begin{aligned}
B(z(w) \circ |\mathcal{B}\rangle) &= -\frac{2}{k^2 W^6} c_1 \tilde{c}_1 |0\rangle \\
&\quad - \frac{1}{k^2 W^4} : c_1 (c_0 + \tilde{c}_0) \tilde{c}_1 B : |0\rangle - \frac{4}{3\pi k^2 W^4} (c_0 + \tilde{c}_0) (\tilde{c}_1 - c_1) |0\rangle \\
&\quad + \frac{2}{W^2} \alpha_{-1} \cdot \tilde{\alpha}_{-1} \tilde{c}_1 c_1 |0\rangle \\
&\quad - \frac{2}{W^2} (c_1 c_{-1} + \tilde{c}_{-1} \tilde{c}_1) |0\rangle - \frac{16}{3\pi W^2} (c_{-1} + \tilde{c}_{-1}) (\tilde{c}_1 - c_1) |0\rangle \\
&\quad - \frac{8}{3\pi W^2} c_0 \tilde{c}_0 |0\rangle + \dots
\end{aligned} \tag{3.31}$$

To see directly how these terms cause the tadpole to diverge, consider for example the term $-\frac{2}{k^2 W^6} c_1 \tilde{c}_1 |0\rangle$, which is the most divergent term in the expansion (3.31). Plugging this term into the expression for $|\mathcal{T}(T)\rangle$ given in equation (3.16) gives

$$\begin{aligned}
|\mathcal{T}(T)\rangle &\sim -\frac{2}{k^2 W^6} U_{h(z) \circ z(v)}^\dagger (h(z) \circ c(0) \tilde{c}(0)) |0\rangle \\
&\propto \frac{e^{2\pi^2/T}}{T^6} U_{h(z) \circ z(v)}^\dagger c(i) \tilde{c}(i) |0\rangle.
\end{aligned} \tag{3.32}$$

As discussed above, as $T \rightarrow 0$ the map $h(z) \circ z(v)$ limits to the map representing the identity state. Thus if we are only interested in $|\mathcal{T}(T)\rangle$ near $T = 0$ we can replace

$$h(z) \circ z(v) = f(v) = \frac{2v}{1-v^2}, \tag{3.33}$$

where $f(z)$ is the usual expression for the identity state in the upper-half plane geometry. Thus we can write, for small T ,

$$|\mathcal{T}(T)\rangle \sim \frac{e^{2\pi^2/T}}{T^6} U_{f(v)}^\dagger c(i) \tilde{c}(i) |0\rangle. \tag{3.34}$$

The full tadpole state is then given by the integral of this state over T . Since the state $U_{f(v)}^\dagger c(i) \tilde{c}(i) |0\rangle$ does not depend on T , the small T region of the integral is determined by the integral over the function $e^{2\pi^2/T}/T$, which diverges. One can also consider what we would get if we take, for example, the term $\frac{2}{W^2} \alpha_{-1} \cdot \tilde{\alpha}_{-1} \tilde{c}_1 c_1 |0\rangle$ from the expansion (3.31). A similar calculation yields

$$|\mathcal{T}(T)\rangle_{\alpha_{-1} \cdot \tilde{\alpha}_{-1} \tilde{c}_1 c_1 |0\rangle} \sim \frac{1}{T^2} U_{f(v)}^\dagger c(i) \partial X^\mu(i) \tilde{c}(i) \bar{\partial} X_\mu(i) |0\rangle, \tag{3.35}$$

where the subscript indicates that this is only the behavior of the terms in $|\mathcal{T}(T)\rangle$ arising from term $\alpha_{-1} \cdot \tilde{\alpha}_{-1} \tilde{c}_1 c_1 |0\rangle$ in the expansion (3.31). Since one cannot integrate $1/T^2$ near zero, this also leads to a divergence in $|\mathcal{T}\rangle$.

For comparisons with the results in section 4, it is useful to note that the expression for the leading divergence of the $|\mathcal{T}(T)\rangle$, given in (3.34), can be rewritten as

$$|\mathcal{T}(T)\rangle \sim \frac{e^{2\pi^2/T}}{T^6} \exp\left(-\frac{1}{2}a_m^\dagger C_{mn} a_n^\dagger - c_m^\dagger C_{mn} b_n^\dagger\right) c_0 c_1 |0\rangle, \quad (3.36)$$

where a_m^\dagger , c_m^\dagger and b_m^\dagger are the usual open string oscillators and $C_{mn} = (-1)^m \delta_{mn}$. Equation (3.36) may be verified using the methods of [32].

3.3 Interpretation of the divergences

The divergences in (3.31) may be interpreted as arising from the propagation of tachyonic and massless closed string modes down a long cylinder. The tube at the bottom of the tadpole is a tube of length $\frac{\pi}{2}$ and circumference T . Rescaling this tube by a factor of $\frac{2\pi}{T}$ gives a tube of length $\frac{\pi^2}{T}$ and constant circumference 2π . These are the standard lengths for closed string theory. If we think of the boundary state at the end of the tube as a closed string state, we may propagate it along the length of the tube using the operator

$$\exp\left(-\frac{\pi^2}{T}(L_0 + \tilde{L}_0)\right). \quad (3.37)$$

For the term in the boundary state given by $c_1(c_0 + \tilde{c}_0)\tilde{c}_1|0\rangle$, which we may think of as coupling to the closed string tachyon, this gives a prefactor of

$$e^{2\pi^2/T} \sim \frac{1}{k^2}. \quad (3.38)$$

For the weight zero terms from the boundary state there is no term picked up from the propagation. However we must account for the measure on the moduli. Taking the modulus to be the length of the cylinder $s = \frac{\pi^2}{T}$, the usual measure on a cylinder is just $ds = -\pi^2 \frac{dT}{T^2}$.

Of course the full tadpole diagram is not just a cylinder. Complicated conformal factors can and do arise from the specific manner in which the cylinder at the bottom of the diagram is attached to the external open string state. Furthermore since the boundary state is not a conformal primary, conformal transformations can mix the behavior of the various terms. This is seen in equation (3.31). The first three terms diverge as $\sim \frac{1}{k^2}$ suggesting that these divergences come from the propagation of the closed string tachyon over the long cylinder. The next four terms diverge as $\sim \frac{1}{T^2}$ suggesting that these terms arise from the massless closed string sector fields. The term $\alpha_{-1} \cdot \tilde{\alpha}_{-1} \tilde{c}_1 c_1 |0\rangle$ is of the right form to correspond to the graviton/dilaton. Since this field does not mix with any of the other fields under the conformal map $z(w)$, there is no ambiguity that this divergence arises purely from the massless sector. The other fields diverging as $1/W^2$, correspond to auxiliary fields. Because these states are not conformal primaries, they mix with the states coupling to the tachyon field. Thus, these divergences may be due in part to the closed string tachyon

The tachyon divergence may be partially treated by an analytic continuation. If we take the weight of the state $c_1(c_0 + \tilde{c}_0)\tilde{c}_1|0\rangle$ to be (h_1, h_1) , we can try to perform the integrals

over the modular parameter with the assumption that $h_1 > 0$. Since the term, $-(c_1 c_{-1} + \tilde{c}_{-1} \tilde{c}_1)(c_0 + \tilde{c}_0)|0\rangle$, mixes with $c_1(c_0 + \tilde{c}_0)\tilde{c}_1|0\rangle$ under conformal maps we must also take this state to have some arbitrary weight (h_2, h_2) . We can then substitute $h_1 = -1$ and $h_2 = 0$ at the end of the calculation. This prescription works for all the terms containing powers of $1/k$. Unfortunately there are subleading terms which contain no factors of $1/k$, but still diverge as badly as $1/W^5$.

These divergences, which mix with the massless divergences, seem to be an unfortunate consequence of the geometry of the Witten diagram. In other versions of string field theory, such as the one discussed in section 5, these divergences do not arise. It is possible that a more sophisticated method for treating these divergences would eliminate them and that we are merely limited by our inability to correctly identify the tachyonic degrees of freedom, since they are encoded in a highly nontrivial fashion in terms of the fundamental open string degrees of freedom. It is also possible, since we are dealing with off-shell physics, that spurious divergences are arising. Such unexpected off-shell physics was found in [11], where extra poles were found in an internal closed string propagator. Fortunately, however, we can eliminate these $1/W^n$ divergences by considering lower dimensional Dp -brane backgrounds, which is the subject of the next section.

3.4 Lower dimensional Dp -branes

Having examined the case of the D25-brane, we turn to the general case of the Dp -brane for $p < 25$. The only change in the analysis we need to make is to replace the boundary state, $|\mathcal{B}\rangle$, with the correct boundary state for a Dp -brane. This state is given by

$$|\mathcal{B}_p\rangle = \exp\left(\sum_{n=1}^{\infty} \mp \frac{1}{n} \alpha_{-n} \cdot \tilde{\alpha}_{-n} - b_{-m} \tilde{c}_{-m} - \tilde{b}_{-m} c_{-m}\right) \int d^{25-p} q_{\perp} e^{-iq_{\perp} \cdot y_{\perp}} |q_{\perp}, q_{\parallel} = 0\rangle, \quad (3.39)$$

where y_{\perp} is the location of the brane, q_{\perp} is the momentum transverse to the brane, and q_{\parallel} is the momentum parallel to the brane. We will set $y_{\perp}^{\mu} = 0$ for convenience. The minus sign in front of the α 's is chosen for Neumann boundary conditions and the plus sign for Dirichlet.

We can now study the divergence structure of the tadpole diagram by studying $B(z(w) \circ |\mathcal{B}_p\rangle)$. Since the sign changes in (3.39) do not affect the divergence structure we need only consider the effect of the momentum dependence. Because it is simpler, we begin with the massless sector. Consider the contribution from the graviton/dilaton.

$$B(z(w) \circ |\mathcal{B}_p\rangle) = \dots - \int d^{25-p} q_{\perp} \left(\frac{kW^2}{1+W^2}\right)^{q_{\perp}^2} \frac{2}{W^2} \alpha_{-1} \cdot \tilde{\alpha}_{-1} c_1 \tilde{c}_1 |q_{\perp}\rangle + \dots \quad (3.40)$$

Note that the factor of $\left(\frac{kW^2}{1+W^2}\right)^{q_{\perp}^2}$ kills the $W \rightarrow 0$ divergence if $q_{\perp}^2 > 0$. To see whether the point $q_{\perp} = 0$ contributes a divergence in the integral, we map this state to a local operator

at i in the upper-half plane using the map $h^{-1}(z)$. This gives the operator

$$\int d^{25-p}q_{\perp} (2)^{q_{\perp}^2} \left(\frac{kW^2}{1+W^2} \right)^{q_{\perp}^2} \frac{2}{W^2} c\partial X(i) \tilde{c}\bar{\partial} X(i) e^{iq_{\perp}\cdot X(i)}. \quad (3.41)$$

In the upper-half plane geometry, the external state is mapped to some local operator at the origin. By Lorentz invariance, this operator cannot have any momentum dependence.

We can now evaluate the tadpole in this geometry using the Green's function relevant to the Dirichlet/Neumann boundary conditions. The term $e^{iq_{\perp}\cdot X(i)}$ produces a factor of $(2)^{-k_{\perp}^2}$ when it contracts with itself. There can also be additional momentum dependent factors when $e^{iq_{\perp}\cdot X(i)}$ contracts with other X 's in the boundary state and in the external state. These will produce additional factors of q_{\perp}^2 . As we will see below, these factors will only make things more convergent, so we can ignore them. If we take just the momentum-dependent and W -dependent terms we get

$$\int d^{25-p}q_{\perp} \left(\frac{kW^2}{1+W^2} \right)^{q_{\perp}^2} \frac{2}{W^2} = \text{Const} \times \int_0^{\infty} dr r^{25-p-1} \left(\frac{kW^2}{1+W^2} \right)^{r^2} \frac{2}{W^2}. \quad (3.42)$$

Dropping the constant from the angular integral, this gives

$$\frac{2}{W^2} \left[-\log \left(\frac{kW^2}{1+W^2} \right) \right]^{\frac{1}{2}(p-25)}. \quad (3.43)$$

Expanding this function around $W = 0$ gives

$$\left(\frac{W}{\pi} \right)^{\frac{25-p}{2}} \frac{1}{W^2} + \mathcal{O}(W^{\frac{25-p-2}{2}}). \quad (3.44)$$

We are interested in when this can be integrated near $W = 0$. Additional factors of W could arise from the external state map but these will only aid the convergence. From the expansion (3.44) we see that we can integrate (3.42) with respect to W near $W = 0$ if

$$p \leq 22. \quad (3.45)$$

Thus, for sufficiently many transverse dimensions, there are no divergences from the massless sector. As we discuss in Section 6, this constraint has a natural interpretation in terms of the long range behavior of the massless fields around the brane.

Now let's look at the tachyon sector. From the calculation in the massless sector, we can see that the only effect of momentum dependence is to give an extra power of $W^{(25-p)/2}$. Unfortunately, this is not enough to suppress the factor of $1/k^2$ so one must still resort to some form of analytic continuation as we did in the D25-brane theory. Unlike the D25-brane case, however, this analytic continuation can now be used to make the diagram completely finite provided p is small enough. Recall that the terms which still diverged after analytic

continuation were at worst of the form $1/W^5$. Thus to make the tadpole integrable around $W = 0$, we must choose $p \leq 16$. While we have a natural interpretation for the constraint (3.45), this additional restriction of the dimensionality of the branes seems to be an artifact of the interplay between our somewhat ad hoc choice of analytic continuation and the details of the Witten OSFT. We do not believe that there is any universal significance to this constraint; indeed, it is not evident in the alternative string field theory discussed in section 5.

As in the D25-brane case, it is instructive to compare these results with the propagation of the boundary state along a closed string tube of length $\frac{\pi}{W}$ and circumference 2π . As before, the propagation of the boundary state is represented by

$$\exp\left(-\frac{\pi}{W}(L_0 + \tilde{L}_0)\right) |\mathcal{B}_p\rangle. \quad (3.46)$$

Consider decomposing the boundary state into a sum over states of definite weight, (h, h) , and momentum, q_\perp ,

$$|\mathcal{B}_p\rangle = \sum_{h=-1}^{\infty} \int d^{25-p} q_\perp |\mathcal{B}_p(q_\perp, h)\rangle. \quad (3.47)$$

We can then write (3.46) as

$$\sum_{h=-1}^{\infty} \int d^{25-p} q_\perp \exp\left(-\frac{\pi}{W}(2h + k_\perp^2)\right) |\mathcal{B}_p(q_\perp, h)\rangle. \quad (3.48)$$

Now consider the different terms in the sum over h . For $h > 0$, the term in the exponent $2h + k_\perp^2$ is always greater than zero. Thus the limit as $W \rightarrow 0$ is well defined. For $h = 0$ the limit $W \rightarrow 0$ is well defined for the region of integration where $q_\perp^2 > 0$. As we saw above, the region of the integral around $q_\perp^2 = 0$ is also defined for sufficiently small p .

For the tachyon, however, we have $h = -1$. Now, whenever $q_\perp^2 < 2$, the limit as $W \rightarrow 0$ is divergent. Thus the added momentum dependence does nothing to help the tachyon divergence and we must resort to analytic continuation.

4. Evaluation of the tadpole using oscillator methods

Having examined the one-point function using conformal field theory methods, we now evaluate it using the oscillator approach of [25]. In this section we primarily specialize to the D25-brane. We will comment on the lower dimensional branes at the end of the section. In section 4.1 we review the oscillator form of the two- and three-string vertices and use squeezed state methods to compute the one-loop tadpole in terms of infinite matrices of Neumann coefficients. In sections 4.2 and 4.3, we analyze the results using numerical and analytical methods and compare with our results from section 3.

4.1 Oscillator description of the one-loop tadpole

We begin by writing an oscillator description for the tadpole diagram, following [8, 25]. The oscillator expressions for the two- and three-string vertices $|V_2\rangle$ and $|V_3\rangle$ are squeezed states in the two-fold and three-fold tensor product of the string Fock space with itself [32, 34, 35, 36, 37, 38, 39]. Explicit formulae for these vertices are given below. In Feynman-Siegel gauge, $b_0|\Psi\rangle = 0$, and the propagator is given by b_0/L_0 , which we can represent using a Schwinger parameter

$$\frac{b_0}{L_0} = b_0 \int_0^\infty dT e^{-TL_0}. \quad (4.1)$$

We can use the vertices and the propagator to write the tadpole as

$$|\mathcal{T}\rangle = -g \int_0^\infty dT {}_{1,2}\langle \tilde{V}_2 | b_0^2 e^{-\frac{1}{2}T(L_0^{(1)} + L_0^{(2)})} |V_3\rangle_{1,2,3}. \quad (4.2)$$

The three-string vertex is given by

$$\begin{aligned} |V_3\rangle = & \int d^{26}p_1 d^{26}p_2 \exp\left(-\frac{1}{2}a_n^{i\dagger} V_{nm}^{ij} a_m^{j\dagger} - a_n^{i\dagger} V_{n0}^{ij} p_j - \frac{1}{2}p_i V_{00}^{ij} p_j\right) \\ & \times \exp\left(-c_n^{i\dagger} X_{nm}^{ij} b_m^{j\dagger}\right) c_0^1|\hat{0}; p_1\rangle_1 c_0^2|\hat{0}; p_2\rangle_2 c_0^3|\hat{0}; p_3 = -p_1 - p_2\rangle_3, \end{aligned} \quad (4.3)$$

where sums on all repeated indices are understood. The vacuum $|\hat{0}\rangle = c_1|0\rangle$, where as before $|0\rangle$ is the $SL(2, \mathbf{R})$ -invariant vacuum. The Neumann coefficients V_{nm}^{ij} and X_{nm}^{ij} are given by standard formulae [34, 35, 39] and are tabulated in [48] among other places. The two-string vertex $|\tilde{V}_2\rangle$ is related to the usual two-string vertex $|V_2\rangle$ through

$$|\tilde{V}_2\rangle = (-1)^{N_g^{(1)}} |V_2\rangle \quad (4.4)$$

and has the following oscillator representation

$$|\tilde{V}_2\rangle = \int d^{26}p (c_0^1 + c_0^2) \exp\left(-a_n^{1\dagger} C_{nm} a_m^{2\dagger} - c_n^{1\dagger} C_{nm} b_m^{2\dagger} - c_n^{2\dagger} C_{nm} b_m^{1\dagger}\right) |\hat{0}; p\rangle_1 |\hat{0}; -p\rangle_2, \quad (4.5)$$

where

$$C_{nm} = \delta_{nm} (-1)^n. \quad (4.6)$$

The extra sign in (4.4) arises from the fact that the b_0 in the propagator anticommutes with Grassmann-odd states in $|V_2\rangle$ [8]. Note that in (4.2) we have used the property

$$e^{-TL_0^{(1)}} |\tilde{V}_2\rangle = e^{-\frac{T}{2}(L_0^{(1)} + L_0^{(2)})} |\tilde{V}_2\rangle \quad (4.7)$$

to make the expression more symmetric.

We may represent the action of the propagator on the vertex by multiplying each term in the vertex by the appropriate function of its conformal weight. That is, since

$[L_0^{(k)}, a_n^{i\dagger} V_{nm}^{ij} a_m^{j\dagger}] = (n\delta_{ik} + m\delta_{jk}) a_n^{i\dagger} V_{nm}^{ij} a_m^{j\dagger}$, we have

$$\begin{aligned} e^{-TL_0^{(k)}} \exp\left(-\frac{1}{2} a_n^{i\dagger} V_{mn}^{ij} a_m^{j\dagger}\right) c_0^1|\hat{0}; 0\rangle_1 c_0^2|\hat{0}; 0\rangle_2 c_0^3|\hat{0}; 0\rangle_3 \\ = e^T \exp\left(-\frac{1}{2} a_n^{i\dagger} V_{mn}^{ij} a_m^{j\dagger} e^{-T(n\delta_{ik} + m\delta_{jk})}\right) c_0^1|\hat{0}; 0\rangle_1 c_0^2|\hat{0}; 0\rangle_2 c_0^3|\hat{0}; 0\rangle_3, \end{aligned} \quad (4.8)$$

with an analogous result in the ghost sector. As in [25], we denote a vertex which has absorbed a propagator in this fashion by a hat, so that

$$\hat{V}_{nm}^{ikjl}(T_k, T_l) \equiv e^{-nT_k/2} V_{nm}^{ikjl} e^{-mT_l/2}. \quad (4.9)$$

Using the explicit representations (4.1, 4.3, 4.5) of the vertices and propagators, the evaluation of $|\mathcal{T}\rangle$ at fixed modular parameter T reduces to computing the inner product of two squeezed states. The formula for squeezed state expectation values is given by [49]

$$\langle 0|e^{-\frac{1}{2}aSa} e^{-\mu a^\dagger - \frac{1}{2}a^\dagger V a^\dagger} |0\rangle = \det(1 - SV)^{-1/2} e^{-\frac{1}{2}\mu(1-SV)^{-1}S\mu}, \quad (4.10)$$

where a and a^\dagger are understood to be vectors, and matrix multiplication is implicit. We also need the corresponding fermionic formula

$$\langle 0|e^{cSb} e^{-\lambda c b^\dagger - c^\dagger \lambda b - c^\dagger X b^\dagger} |0\rangle = \det(1 - SX) e^{-\lambda c(1-SX)^{-1}S\lambda_b} \quad (4.11)$$

where we have suppressed the ghost zero mode dependence.

We now apply these formulas to the tadpole. Since the diagram factorizes into separate matter and ghost portions, we will discuss the matter and ghost parts in turn. The matter portion of the expectation value in the integrand of (4.2) is given by

$$\int d^{26}q e^{-T(q^2-1)-q^2V_{00}^{11}} {}_{1,2}\langle 0|e^{-\frac{1}{2}aSa} e^{-\frac{1}{2}a^\dagger \tilde{V} a^\dagger - \mu a^\dagger - \frac{1}{2}a^{3\dagger} V^{11} a^{3\dagger}} |0\rangle_{1,2,3}, \quad (4.12)$$

where we have defined

$$S = \begin{pmatrix} 0 & C \\ C & 0 \end{pmatrix}, \quad (4.13)$$

$$\tilde{V} = \begin{pmatrix} \hat{V}^{11}(T, T) & \hat{V}^{12}(T, T) \\ \hat{V}^{21}(T, T) & \hat{V}^{11}(T, T) \end{pmatrix}, \quad (4.14)$$

$$\mu = \begin{pmatrix} \hat{V}^{21}(T, 0) \\ \hat{V}^{12}(T, 0) \end{pmatrix} a^{3\dagger} + \begin{pmatrix} \hat{V}_{n0}^{11}(T, 0) - \hat{V}_{n0}^{12}(T, 0) \\ \hat{V}_{n0}^{21}(T, 0) - \hat{V}_{n0}^{11}(T, 0) \end{pmatrix} q. \quad (4.15)$$

Using the squeezed state formula (4.10) and carrying out the resulting Gaussian integral over momentum (with the appropriate analytic continuation), equation (4.12) becomes

$$e^T \left(\frac{2\pi}{Q \det(1 - S\tilde{V})} \right)^{13} \exp\left(-\frac{1}{2} a_n^\dagger M_{nm} a_m^\dagger\right) |0\rangle, \quad (4.16)$$

where

$$\begin{aligned}
M_{nm} &= Q_{nm} - \frac{Q_n Q_m}{Q}, \\
Q_{nm} &= V_{nm}^{11} + \left(\begin{array}{c} \hat{V}_{n\cdot}^{12}(0, T) \\ \hat{V}_{n\cdot}^{21}(0, T) \end{array} \right)^T \frac{1}{1 - S\tilde{V}} S \left(\begin{array}{c} \hat{V}_{\cdot m}^{21}(T, 0) \\ \hat{V}_{\cdot m}^{12}(T, 0) \end{array} \right), \\
Q_n &= V_{0n}^{13} - V_{0n}^{23} + \left(\begin{array}{c} \hat{V}_{0\cdot}^{11}(0, T) - \hat{V}_{0\cdot}^{21}(0, T) \\ \hat{V}_{0\cdot}^{12}(0, T) - \hat{V}_{0\cdot}^{11}(0, T) \end{array} \right)^T \frac{1}{1 - S\tilde{V}} S \left(\begin{array}{c} \hat{V}_{\cdot n}^{21}(T, 0) \\ \hat{V}_{\cdot n}^{12}(T, 0) \end{array} \right), \\
Q &= 2V_{00}^{11} + 2T + \left(\begin{array}{c} \hat{V}_{0\cdot}^{11}(0, T) - \hat{V}_{0\cdot}^{21}(0, T) \\ \hat{V}_{0\cdot}^{12}(0, T) - \hat{V}_{0\cdot}^{11}(0, T) \end{array} \right)^T \frac{1}{1 - S\tilde{V}} S \left(\begin{array}{c} \hat{V}_{\cdot 0}^{11}(T, 0) - \hat{V}_{\cdot 0}^{12}(T, 0) \\ \hat{V}_{\cdot 0}^{21}(T, 0) - \hat{V}_{\cdot 0}^{11}(T, 0) \end{array} \right).
\end{aligned} \tag{4.17}$$

Meanwhile, the ghost portion of the expression (4.2) is

$${}_{1,2}\langle 0 | e^{cSb} e^{-c^\dagger \tilde{X} b^\dagger - \lambda_c b^\dagger - c^\dagger \lambda_b - c^{3\dagger} X^{11} b^{3\dagger}} | 0 \rangle_{1,2,3}, \tag{4.18}$$

with

$$\begin{aligned}
\tilde{X} &= \begin{pmatrix} \hat{X}^{11}(T, T) & \hat{X}^{12}(T, T) \\ \hat{X}^{21}(T, T) & \hat{X}^{11}(T, T) \end{pmatrix}, \\
\lambda_c &= c^{\dagger 3} \begin{pmatrix} \hat{X}^{12}(0, T) & \hat{X}^{21}(0, T) \end{pmatrix}, \\
\lambda_b &= \begin{pmatrix} \hat{X}^{21}(T, 0) \\ \hat{X}^{12}(T, 0) \end{pmatrix} b^{\dagger 3} + \begin{pmatrix} \hat{X}_{n0}^{21}(T, 0) \\ \hat{X}_{n0}^{12}(T, 0) \end{pmatrix} b_0^3.
\end{aligned} \tag{4.19}$$

Using the squeezed state formula (4.11), we find

$$\det(1 - S\tilde{X}) \exp(-c_n^\dagger R_{nm} b_m^\dagger) c_0 |\hat{0}\rangle, \tag{4.20}$$

where we have defined

$$R = X^{11} + \left(\begin{array}{cc} \hat{X}^{12}(0, T) & \hat{X}^{21}(0, T) \end{array} \right) \frac{1}{1 - S\tilde{X}} S \left(\begin{array}{c} \hat{X}^{21}(T, 0) \\ \hat{X}^{12}(T, 0) \end{array} \right). \tag{4.21}$$

Up to an overall constant, then, $|\mathcal{T}\rangle$ is given by,

$$|\mathcal{T}\rangle = \int_0^\infty dT e^T \frac{\det(1 - S\tilde{X})}{(Q \det(1 - S\tilde{V}))^{13}} e^{-\frac{1}{2} a^\dagger M a^\dagger - c^\dagger R b^\dagger} c_0 |\hat{0}\rangle. \tag{4.22}$$

4.2 Divergences in the tadpole

We are now interested in evaluating the tadpole integral (4.22). At any finite value of T , the integrand is a state in the string Fock space with finite coefficients for each zero-momentum state. The matrices X_{nm}^{rs} and V_{nm}^{rs} are infinite-dimensional, and while we have expressions for

each matrix element, we cannot analytically compute the integrand of (4.22). Nonetheless, by truncating the matrices X and V at finite oscillator level, we can numerically estimate the value of the integrand. Empirical evidence indicates that the integrand converges exponentially quickly as the level of truncation is increased, where the rate of convergence depends on the modular parameter T . For large T , we can also consider expanding (4.22) as a function of e^{-T} . The contribution at order $e^{(1-k)T}$ represents the portion of the tadpole arising from the propagation of open string states at level k around the loop.

It is immediately clear from (4.22) that the integral for the tadpole diverges as $T \rightarrow \infty$ due to the term of order e^T . This term arises from the propagation of the open string tachyon around the loop. In an expansion in terms of the level of the field propagating around the loop, it is easy to see how this divergence can be removed by analytic continuation. Unlike the divergence from the closed string tachyon considered in the CFT calculation, the field causing this divergence is explicitly considered as one of the fundamental degrees of freedom in OSFT, and thus the associated tachyon divergence can easily be removed by analytic continuation. This analytic continuation is most transparent when we do the calculation level by level in fields. The method of level truncation by fields has previously been used in many OSFT calculations, and is probably the most effective way of dealing with the open string tachyon; because we are more interested in closed string physics here, however, we will not pursue this approach further and we will instead approximate (4.22) by truncation in oscillator level, which leads to a simpler calculation of the integrand at small T .

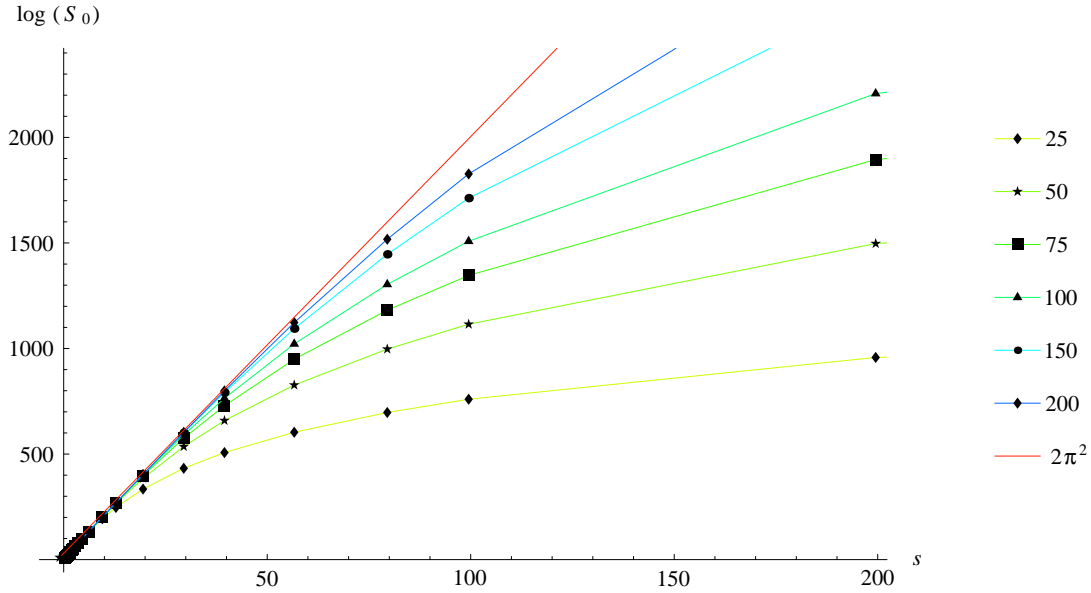


Figure 6: $\log S_0$ vs. $s = 1/T$. The straight line plotted has a slope of $2\pi^2$, which is the analytical prediction from section 3.

From the CFT analysis, we expect to see a divergence in the integrand of (4.22) as $T \rightarrow 0$. Indeed, we see numerical evidence for such a divergence. Let us first consider the

scalar portion of the state (4.22),

$$S_0(T) = e^T \frac{\det(1 - S\tilde{X})}{\det(1 - S\tilde{V})^{13} Q^{13}}. \quad (4.23)$$

Our numerical computations of S_0 are plotted in figure 6. We find that as $T \rightarrow 0$, S_0 first increases exponentially, and then falls off, taking a finite value at $T = 0$. Both aspects of this behavior have simple explanations. The exponential increase is the divergence arising from the negative mass-squared of the closed string tachyon, and takes the form $S_0 \propto e^{B/T}$. We can compute the coefficient B numerically, as we discuss below. The fall-off occurs because as $T \rightarrow 0$ we consider smaller and smaller world-sheet distances, which require higher and higher oscillator modes to resolve. Level truncation essentially acts as a UV cutoff, rendering the divergence finite as $T \rightarrow 0$.

From the conformal field theory analysis, we expect that if we could compute $S_0(T)$ to infinite level we would find

$$S_0(T) \sim e^{2\pi^2/T}. \quad (4.24)$$

In figure 6 we plot the quantity $\log S_0$ versus $s = 1/T$ at successively higher levels. The straight line with slope $2\pi^2$ is the CFT prediction for the infinite level behavior in the region $s \gg 1$. As is evident from the plot, our numerical data is in good accord with this prediction. As expected, as the level increases the region of linear behavior becomes larger, while the fall-off becomes less rapid, so that successively better estimations of B are obtained.

Our data, considered as a function of level, converges exponentially quickly; that is, to a good approximation, we may write the amplitude obtained at finite level as

$$\log S_0^{(L)}(T) = \log S_0^{(exact)}(T) - Ae^{-r(T)L}, \quad (4.25)$$

where L is the level. The rate of convergence $r(T)$ is approximately given by

$$r(T) \approx 0.002 + 0.949 T. \quad (4.26)$$

This approximation to the function $r(T)$ is obtained by numerically determining the rate of convergence for several points at fixed values of T using the ansatz $r(T) = A + BT$. Since the first terms dropped in the level L truncation are of order e^{-LT} , we indeed expect $r(T) = T$, in close agreement with our empirical data. These results are consistent with the general empirical observation that, while integrated amplitudes converge polynomially in $1/L$ (when finite), the integrand itself converges exponentially in L with a rate that depends on the modular parameter [25].

Looking at the region $T > .007$, we find the best fit given by equations (4.25) and (4.26) gives

$$B \approx .9911 \times 2\pi^2. \quad (4.27)$$

This is within less than 1% of the value $2\pi^2$ found analytically in section 3, so we have a very strong agreement between our two methods of calculation for the leading rate of divergence.

4.3 The matrices M and R

In this subsection, we consider the form of the matrices M and R in the exponential part of (4.22). We show that in the limit $T \rightarrow 0$, these matrices reduce to C_{nm} , so that just as in the CFT calculation, the leading divergence is associated with a Shapiro-Thorn state. Furthermore, we compute the first subleading terms in M and R . We show that these subleading terms agree with what is expected from the CFT calculation.

In the small T limit, the loop of the tadpole diagram reduces to an identification of the left and right halves of the incoming string. Therefore, the matrices $M_{nm} = Q_{nm} + Q_n Q_m / Q$ and R_{nm} should both limit to C_{nm} in order to describe the identification of the sides of the string. For any finite level, we can demonstrate analytically that this is indeed the case for the matrix M of (4.18) and R of (4.21). Consider the identity

$$\begin{pmatrix} J_2 & J_3 \end{pmatrix} \begin{pmatrix} 1 - CJ_3 & -CJ_1 \\ -CJ_1 & 1 - CJ_2 \end{pmatrix}^{-1} = \begin{pmatrix} C & C \end{pmatrix} \quad (4.28)$$

which holds for any matrices J_i that satisfy $J_1 + J_2 + J_3 = C$.

In level truncation, we can simply apply the identity (4.28) at $T = 0$, with J_i equal to X^{1i} and V^{1i} in the ghost and matter sectors respectively. This gives us the result

$$\begin{aligned} R_{nm}(T = 0) &= C_{nm} \\ M_{nm}(T = 0) &= C_{nm}. \end{aligned} \quad (4.29)$$

Since the sum condition needed to demonstrate this result is linear, we find that $M(T = 0)$ and $R(T = 0)$ are equal to C level by level when we calculate them in level truncation. This reproduces the formula we found in equation (3.36). Unfortunately, one can show that there is no analogue of equation (4.28) without level truncation. This makes the verification of (4.29) without truncating the matrices quite difficult. We discuss some of the subtleties of comparing the level truncated analysis and the infinite dimensional matrix analysis in appendix B.

We can also look at the first order corrections to M_{nm} and R_{nm} . Doing a linear fit near $T = 0$ to the various coefficients gives for the first five diagonal elements at level 25,

$$\begin{aligned} M_{11} &\approx -0.9999999 + 1.0000031 (T) \\ M_{22} &\approx 0.9999994 - 1.0000095 (2T) \\ M_{33} &\approx -0.9999982 + 1.0000265 (3T) \\ M_{44} &\approx 0.9999953 - 1.0000349 (4T) \\ M_{55} &\approx -0.9999912 + 1.0000694 (5T). \end{aligned} \quad (4.30)$$

The off diagonal elements are consistent with being zero to $\mathcal{O}(T)$. We find similar behavior in the ghost sector. At level 150 we find the following coefficients for a linear fit near $T = 0$

$$\begin{aligned}
R_{11} &\approx -0.999995 + 0.999775 (T) \\
R_{22} &\approx 0.999989 - 0.999642 (2T) \\
R_{33} &\approx -0.999985 + 0.999761 (3T) \\
R_{44} &\approx 0.999979 - 0.999627 (4T) \\
R_{55} &\approx -0.999975 + 0.999741 (5T).
\end{aligned} \tag{4.31}$$

As with the matter sector, the off diagonal elements are approximately zero to $\mathcal{O}(T)$.

These coefficients suggest that the first order corrections to M_{nm} and R_{nm} are given by

$$\begin{aligned}
M_{nm} &= C_{nm} - mC_{nm} T + \mathcal{O}(T^2) \\
R_{nm} &= C_{nm} - mC_{nm} T + \mathcal{O}(T^2).
\end{aligned} \tag{4.32}$$

It might seem that this formula should be easy to derive by just Taylor expanding the expressions for M_{nm} and R_{nm} to first order in T . In level truncation, this expansion is straightforward and yields the result

$$\begin{aligned}
M_{nm}^L &= C_{nm} - 2mC_{nm} T + \mathcal{O}(T^2) \\
R_{nm}^L &= C_{nm} - 2mC_{nm} T + \mathcal{O}(T^2),
\end{aligned} \tag{4.33}$$

where we have put the superscript L in the matrices to emphasize that this expression is only valid in level truncation. Note that equations (4.32) and (4.33) are off by a factor of two! This disagreement stems from the fact that one must take the level to infinity and then expand around $T = 0$. Expanding around $T = 0$ and then taking the level to infinity gives incorrect results. For a more complete discussion of this issue see appendix B.

We can now compare (4.32) with our results from the conformal field theory method. As it turns out the linear correction comes entirely from the map that acts on the external state. The corrections that arise from the map that acts on the boundary state only enter at $\mathcal{O}(T^2)$. Using the notation of section 3.2 we can write the external state map as $f(z) = h(z) \circ z(v)$. At $T = 0$, $f(z)$ is just the map corresponding to the identity state

$$f(z)\Big|_{T=0} = \frac{2z}{1-z^2}. \tag{4.34}$$

As it turns out, the first order correction in T takes a simple form

$$f(z) = f(z)\Big|_{T=0} \circ \left(\frac{z}{1+T/2} \right) + \mathcal{O}(T^2). \tag{4.35}$$

Thus to $\mathcal{O}(T)$ we can write

$$f(z) \circ |A\rangle = f(z)\Big|_{T=0} \circ \left(\frac{z}{1+T/2} \right) \circ |A\rangle. \tag{4.36}$$

Since we also have

$$\left(\frac{z}{1+T/2}\right) \circ |A\rangle = (1+T/2)^{-L_0}|A\rangle, \quad (4.37)$$

the change in the tadpole state from this correction to the external state map can be accounted for by just taking

$$|\mathcal{T}\rangle\Big|_{T=0} \rightarrow (1+T/2)^{-L_0} \left(|\mathcal{T}\rangle\Big|_{T=0}\right) + \mathcal{O}(T^2), \quad (4.38)$$

where we are only setting $T = 0$ in the map from the external state to the geometry. Acting with $(1+T/2)^{-L_0}$ on an arbitrary state is straightforward since one just takes, for example,

$$a_m^\dagger \rightarrow (1+T/2)^{-m} a_m^\dagger, \quad (4.39)$$

and similarly for the ghosts. Thus the terms in the exponent become

$$\begin{aligned} -\frac{1}{2}a_m^\dagger C_{mn} a_n^\dagger - c_m C_{mn} b_n &\rightarrow -\frac{1}{2}(1+T/2)^{-2m} a_m^\dagger C_{mn} a_n^\dagger - (1+T/2)^{-2m} c_m^\dagger C_{mn} b_n^\dagger \\ &= -\frac{1}{2}a_m^\dagger (C_{mn} - mT C_{mn}) a_n^\dagger - c_m^\dagger (C_{mn} - mT C_{mn}) b_n^\dagger + \mathcal{O}(T^2), \end{aligned}$$

which reproduces what we found in equations (4.32).

4.4 Summary of oscillator calculation

We have given an analytic expression for the tadpole in terms of infinite-dimensional matrices of Neumann coefficients. A divergence associated with the open string tachyon arises for large Schwinger parameter T , and can be dealt with by straightforward analytic continuation when the amplitude is expanded in the level of the open string field propagating in the loop. We have numerically analyzed the behavior of the tadpole integrand as $T \rightarrow 0$. Our numerical approximations have reproduced to a high degree of accuracy the leading divergence in this limit. Near $T = 0$ the tadpole takes the form

$$|\mathcal{T}\rangle \sim \int_0 dT e^{2\pi^2/T} e^{-\frac{1}{2}a^\dagger C a^\dagger - c^\dagger C b^\dagger} |0\rangle + \dots \quad (4.40)$$

This leading term is the zero-momentum Shapiro-Thorn state $|\Phi\rangle = e^{-\frac{1}{2}a^\dagger C a^\dagger - c^\dagger C b^\dagger} |0\rangle$ that describes the closed-string tachyon [12, 13]. The oscillator calculation thus agrees with the conformal calculation of section 3.

We have also identified the leading corrections (in T) to the limit $M, R = C$. These corrections are linear in T and do not represent Shapiro-Thorn states for massless closed string fields. In terms of the conformal calculation discussed in the previous section, these corrections may be understood as coming from the conformal transformation of the incoming string.

Ideally we would like to be able to see the Shapiro-Thorn states for the graviton and dilaton. These could arise from terms in M that vanish as $e^{-2\pi^2/T}$ as $T \rightarrow 0$; such terms

can give a finite contribution to the amplitude because of the exponential divergence in the scalar portion of the amplitude S_0 . However, such exponentially dying corrections are not only many orders of magnitude smaller than the leading corrections, but also many orders of magnitude smaller than the error introduced by level truncation. Without analytic control over the matrices \tilde{V} and \tilde{X} or some way of explicitly removing the divergence due to the closed string tachyon, we cannot examine the subleading terms directly in numerical experiments.

Finally, we note that it would be easy to redo the calculations for the lower-dimensional branes. We would simply introduce a few minus signs for the Dirichlet coordinates and eliminate the momentum integrals for the transverse directions. Without some new approach to the calculation, however, all we would find is the same divergence from the closed string tachyon. We would not be able to observe that the massless sector was no longer contributing to the divergence.

5. The open string tadpole in open-closed string field theory

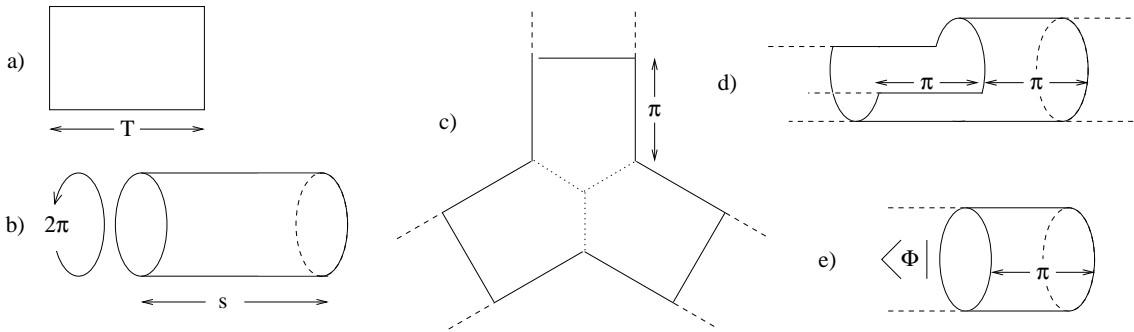


Figure 7: The relevant vertices in OCSFT. a) The open string propagator is the same as in OSFT. b) The closed string propagator is a tube of circumference 2π . Its length, s , is integrated from 0 to ∞ . c) The open string vertex is similar to the OSFT vertex but world-sheet stubs of length 2π are added on each side. d) The open-closed string transition vertex represents an open string which turns in into a closed string. e) The vertex representing a closed string being absorbed by the brane.

To understand the physics hidden in the OSFT tadpole, it is useful to study the same diagram in a version of string field theory which includes closed strings explicitly. This open-closed string field theory (OCSFT), due to Zwiebach [50, 51], has the nice property that it divides up moduli space so that there are never any pinched-off world-sheets. This is convenient for us, since it implies that in this theory the tube at the bottom of the OSFT tadpole will be explicitly written as a closed string propagator. For a related discussion in a different version of string field theory, see [52].

OCSFT is complicated by the fact that its action is non-polynomial but, since we are working only to order g , we will only need to consider a few terms. In fact since we are only interested in the divergent part of the tadpole, we truncate the theory to just the terms in

the action relevant to the $T \rightarrow 0$ part of the tadpole moduli space. These terms may be summarized as follows

1. Start with the usual OSFT action but modify the cubic term by adding to the vertex strips of length π to each of the three sides. The resulting vertex is shown in figure 7 c. The stubs added to the Witten vertex eliminate the region of the tadpole near $T \rightarrow 0$.
2. Add to the theory a set of closed string fields Φ with kinetic term $\langle \Phi | (c_0 - \tilde{c}_0) (Q_B + \tilde{Q}_B) | \Phi \rangle$. The field Φ is assumed to satisfy $(b_0 - \tilde{b}_0) \Phi = 0$. We also impose the analogue of FS gauge $(b_0 + \tilde{b}_0) \Phi = 0$. The propagator of the theory is given by integrating over closed string tubes of length s with insertions of $b_0 \tilde{b}_0$.
3. Add the open-closed string vertex shown in figure 7 d. We will denote this vertex $\langle V_{\text{OC}} | | \Psi \rangle | \Phi \rangle$.
4. Add a vertex in which a closed string is absorbed by the brane. This is given by $\langle \Phi | (c_0 - \tilde{c}_0) e^{-\pi(L_0 + \tilde{L}_0)} | \mathcal{B} \rangle$. Pictorially this vertex is shown in figure 7 e.

We can now consider the OCSFT version of the open string tadpole. Using the new open string vertex in figure 7 c, and the open string propagator one can construct a tadpole diagram that looks just like the one we considered on OSFT. The only difference is that because of the stubs, the loop cannot have length $T < 2\pi$. The part of the tadpole moduli space near $T \rightarrow 0$ is covered by a new diagram formed by gluing an open string propagator to an open-closed vertex, then attaching a closed string propagator and finally capping the diagram with the vertex in figure 7 e. The resulting diagram is pictured in figure 8.

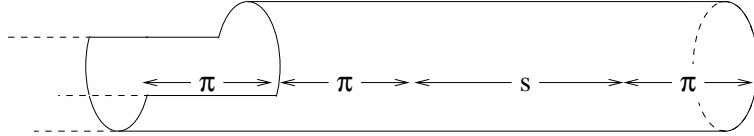


Figure 8: The OCSFT representation of the open string tadpole.

Note that the dependence on s is quite simple since it is just the propagation of the boundary state a distance s . Thus everything to the right of the open-closed vertex can be represented as

$$(b_0 + \tilde{b}_0) \int_{\pi}^{\infty} ds' e^{-s'(L_0 + \tilde{L}_0)} | \mathcal{B} \rangle. \quad (5.1)$$

As in the OSFT version of the tadpole, this integral diverges because of the weight $(-1, -1)$ field in $| \mathcal{B} \rangle$. As in OSFT we can treat this divergence by analytic continuation in the weight of the tachyon field. This analytic continuation is equivalent to the replacement

$$(b_0 + \tilde{b}_0) \int_{\pi}^{\infty} ds' e^{-s'(L_0 + \tilde{L}_0)} | \mathcal{B} \rangle = \frac{b_0 + \tilde{b}_0}{L_0 + \tilde{L}_0} e^{-\pi(L_0 + \tilde{L}_0)} | \mathcal{B} \rangle \quad (5.2)$$

where the operator $(L_0 + \tilde{L}_0)^{-1}$ is defined on all states that are not weight $(0, 0)$. This analytic continuation is closer in spirit to the analytic continuation used in Section 4 to remove the open string tachyon divergence than the analogous analytic continuation used in Section 3 to deal with the closed string tachyon, since the closed string tachyon is explicitly included among the fundamental degrees of freedom in OCSFT. We can also have divergences from the massless sector, but as we showed for the OSFT tadpole, these are only relevant for the D25, D24 and D23-branes and we postpone discussion of these cases until the end of the section.

Now consider our truncated action (we drop the open string three-vertex since it is not relevant here)

$$S[\Psi, \Phi] = \frac{1}{2} \int \Psi \star Q_B \Psi + \frac{1}{2} \langle \Phi | (c_0 - \tilde{c}_0) (Q_B + \tilde{Q}_B) | \Phi \rangle + g \langle V_{\text{OC}} | | \Psi \rangle | \Phi \rangle + \langle \Phi | (c_0 - \tilde{c}_0) e^{-\pi(L_0 + \tilde{L}_0)} | \mathcal{B} \rangle. \quad (5.3)$$

Note that the closed string tadpole appears even at the classical level. We can try to shift the closed string field by $\Phi \rightarrow \Phi + \delta\Phi$ to cancel this tadpole. This gives

$$\delta S[\Psi, \Phi] = g \langle V_{\text{OC}} | | \Psi \rangle | \delta\Phi \rangle + \langle \Phi | (c_0 - \tilde{c}_0) (Q_B + \tilde{Q}_B) | \delta\Phi \rangle + \text{const.} \quad (5.4)$$

Notice that if we can find a $\delta\Phi$ such that $(Q_B + \tilde{Q}_B) | \delta\Phi \rangle = -e^{-\pi(L_0 + \tilde{L}_0)} | \mathcal{B} \rangle$, then the closed string tadpole will be canceled. We then get the new action

$$S[\Psi, \Phi + \delta\Phi] = \frac{1}{2} \int \Psi \star Q_B \Psi + \frac{1}{2} \langle \Phi | (c_0 - \tilde{c}_0) (Q_B + \tilde{Q}_B) | \Phi \rangle + g \langle V_{\text{OC}} | | \Psi \rangle | \Phi \rangle + g \langle V_{\text{OC}} | | \Psi \rangle | \delta\Phi \rangle. \quad (5.5)$$

Notice that the closed string tadpole is now eliminated, but there is now a new contribution to the open string tadpole.

Let's recalculate the open string tadpole in the shifted theory. The original diagram that we calculated before is now gone because the closed string tadpole (which made up the right half of the diagram) has been canceled. However, there is a new diagram coming from the term $g \langle V_{\text{OC}} | | \Psi \rangle | \delta\Phi \rangle$. This diagram may be thought of as the original open string tadpole, but with the closed string propagator chopped off and the state $-\delta\Phi$ stuck onto the end. Note that since this diagram has no closed string modulus to integrate, it is finite as long as $|\delta\Phi\rangle$ is finite. This fact will be useful for us when we discuss the cases where we have divergences from the massless sector in the original tadpole.

Now, as discussed in [26], the equation $(Q_B + \tilde{Q}_B) | \Phi \rangle = -e^{\pi(L_0 + \tilde{L}_0)} | \mathcal{B} \rangle$ is equivalent to the linearized Einstein's equations in the background of the brane. Thus the new open string tadpole represents a coupling between the closed string background and the open strings.

For OSFT this may not seem important since there is no closed string background to shift. However, what makes this discussion relevant for OSFT is that the open string tadpole

after the shift in the closed string background is actually equal to the open string tadpole before we made the shift. This is seen by solving the equation for $|\Phi\rangle$ to get

$$|\Phi\rangle = -\frac{b_0 + \tilde{b}_0}{L_0 + \tilde{L}_0} e^{\pi(L_0 + \tilde{L}_0)} |\mathcal{B}\rangle. \quad (5.6)$$

Thus, replacing the closed string propagator with $-|\Phi\rangle$ is equivalent to doing nothing. The implication for the open string tadpole in OSFT is that as long as the diagram is finite it naturally incorporates the linearized shift in the closed string background.

This leads to the question: what can we say about the tadpole diagrams which diverge because of the massless sector? For the finite diagrams the closed string propagator essentially represents the inverse of the BRST operator. For the divergent diagrams this representation is not defined when acting on the boundary state. To cure this problem one must invert the BRST operator by hand. To see how this is done it is useful to note how BRST invariance is maintained in the shifted and unshifted theory. Recall that in string theory BRST invariance for scattering diagrams reduces to the fact that exact states should decouple from on-shell states. For the tadpole diagram this simply implies that the tadpole should be annihilated by the BRST operator.

In the unshifted theory, when $Q_B + \tilde{Q}_B$ is pulled through the OCSFT tadpole diagram, it picks a contribution from the closed string propagator given by

$$\begin{aligned} \int_{\pi}^{\infty} ds' \{Q_B + \tilde{Q}_B, b_0 + \tilde{b}_0\} e^{-s'(L_0 + \tilde{L}_0)} |\mathcal{B}\rangle &= \int_{\pi}^{\infty} ds' (L_0 + \tilde{L}_0) e^{-s'(L_0 + \tilde{L}_0)} |\mathcal{B}\rangle \\ &= - \int_{\pi}^{\infty} ds' \frac{\partial}{\partial T} e^{-s'(L_0 + \tilde{L}_0)} |\mathcal{B}\rangle \\ &= - e^{-s'(L_0 + \tilde{L}_0)} \Big|_{s=\pi}^{\infty} |\mathcal{B}\rangle. \end{aligned} \quad (5.7)$$

As with the open string, we only pick up contributions at the endpoints of integration. The contribution at $s = \pi$ cancels with a surface term from a part of the tadpole moduli space that we haven't included.

In the shifted theory, we have replaced the closed string propagator with a surface term. Acting on the surface term with $Q_B + \tilde{Q}_B$ we get

$$-(Q_B + \tilde{Q}_B) |\delta\Phi\rangle = e^{-\pi(L_0 + \tilde{L}_0)} |\mathcal{B}\rangle, \quad (5.8)$$

which is the same surface term at $s = \pi$ that we found in (5.7). Note, though, that (5.8) is the same equation that we used to find $|\Phi\rangle$ in the first place. Thus the condition for BRST invariance essentially determines the surface term.

This fact is quite useful for studying the tadpole for the cases where it diverges. If we take one of the OSFT tadpoles which diverges, we can remove the small T region of integration and replace it with a surface term. By the above discussion, this surface term is mostly determined by BRST invariance. We will employ this fact in section 6.3 where we study the physics hidden in the divergent diagrams.

6. Divergences and closed strings

In this section we discuss the various divergences which arise in the one-loop tadpole as $T \rightarrow 0$, and the role which closed strings play in the structure of the tadpole. In subsection 6.1 we discuss the leading divergence in the tadpole and the closed string tachyon which is responsible for this divergence. In subsection 6.2 we discuss the massless closed string modes and the piece of the tadpole arising from them. In subsection 6.3 we study the physics hidden in the divergent diagrams using BRST invariance. Finally, in subsection 6.4 we discuss some further problems which arise at two loops in OSFT.

6.1 The leading divergence and the closed string tachyon

In both the conformal field theory and oscillator calculations, we found a leading divergence in the open string tadpole which arises from the region of the modular integration near $T = 0$. In terms of the dual parameter $s = \pi^2/T$, the divergence arises from an integral of the form

$$\int^{\infty} ds \left[e^{2s} \exp\left(-\frac{1}{2}a^\dagger \cdot C \cdot a^\dagger - c^\dagger \cdot C \cdot b^\dagger\right) |0\rangle + \text{subleading terms} \right]. \quad (6.1)$$

This divergent type of integral is a standard problem when we have a Schwinger parameter associated with a tachyonic state. In principle, we would like to simply analytically continue the integral, using

$$\int_{\lambda}^{\infty} e^{as} ds \rightarrow -\frac{1}{a} e^{a\lambda}. \quad (6.2)$$

Since the closed string channel associated with the divergent integral is not included explicitly in OSFT, however, it is rather subtle to carry out an analytic continuation of this type. In the CFT calculation, we can do this explicitly once we have expanded around $T = 0$ as in (3.31). As suggested in Section 3, the terms in the small T expansion associated with the tachyon component of the boundary state can be separately analytically continued. Even here, however, we run into difficulties, and have to resort to considering lower dimensional branes to ensure a completely finite diagram.

Moreover, the expansion around $T = 0$ is a difficult starting point for any exact or approximate calculation of the complete tadpole diagram. In order to get a numerical approximation to the tadpole amplitude including the analytic continuation for the closed string tachyon, it is necessary to break the modular integral into several parts. The integral for $T > T_0$ is finite (after the open string tachyon is analytically continued as discussed in Section 4), and can in principle be computed approximately using level truncation on fields in the oscillator formalism. The integral for $T < T_0$ can be approximately computed when T_0 is small using the small T expansion and an explicit analytic continuation of the tachyon term. While this approach allows us to deal with the divergence from the closed string tachyon “by hand” in the particular diagram considered here, we should emphasize

that this method is not general, and for higher-loop diagrams it is much more difficult to see how analogous divergences can be controlled.

In the oscillator approach, it is even less clear how the divergence from the closed string tachyon can be treated. Since level truncation regulates the divergence, the region of the modular integral near $T = 0$ is softened, and the divergent piece cannot be precisely isolated. It seems that in the level-truncated theory, unlike in the CFT picture, there is no way to implement by hand an analytic continuation to deal with the closed string divergence. For this reason, we cannot use the oscillator approach to study other parts of the tadpole, such as the finite part and the part depending on massless closed strings. While this is unfortunate, this problem is an artifact of the closed string tachyon. It seems likely that in superstring field theory, this problem would not occur, so that the oscillator method would be a much more useful approach for analyzing detailed features of loop amplitudes.

It is also worth pointing out at this point that a small modification of the usual formulation of OSFT might make the closed string tachyon divergence much more tractable. If we were to explicitly formulate OSFT in terms of a Lorentzian world-sheet, the real Schwinger parameterization used here could be replaced by an integral with an imaginary exponent. Unlike the divergent integral $\int e^{as}$, the complex integral $\int e^{ias}$ is oscillatory. With such an oscillatory integrand, level truncation should simply suppress the integrand at large values of s , effectively regulating the theory and giving a finite result for integrals which diverge in the Euclidean formulation. Unlike the *ad hoc* approach used to implement analytic continuation in the CFT calculation of the tadpole, this approach would immediately generalize to all diagrams, and would in one stroke deal with the open string tachyon as well as the closed string tachyon. We will not pursue this approach further here, but it is an interesting possible avenue for further investigations.

6.2 Tadpole contributions from massless closed strings

Let us now turn our attention to the massless closed string modes. As mentioned in the previous subsection, the terms in the tadpole arising from these modes cannot be seen in the oscillator calculation without a new formulation of the theory. These terms do appear explicitly, however, in the small T expansion of the tadpole (3.35).

To understand the structure of the terms associated with massless closed strings it is helpful to consider the schematic form of the OCSFT calculation from Section 5. In OCSFT, it is clear that the open string tadpole arises directly from the closed string tadpole. The closed string tadpole in turn encodes the structure of the D-brane as a source for the closed string fields. The D-brane boundary state $|\mathcal{B}\rangle$ only couples to the closed string fields. If we forget about the open strings and solve the equations of motion for the closed string, the linearized equation of motion corresponds to the linearized gravity equations in the presence of the brane. For a Dp -brane source, the linearized gravitational equations take the schematic

form

$$\partial^2 \phi(x) = \delta^{25-p}(x_\perp). \quad (6.3)$$

(We ignore here the details of the tensor structure of the full gravity multiplet in order to elucidate the underlying physics; the exact equations for the gravitational fields are written in the following subsection.) In momentum space, the solution of (6.3) is

$$\phi(k) = \frac{1}{k_\perp^2} \delta(k_\parallel). \quad (6.4)$$

In position space, the solution is just the usual

$$\phi(x) \propto r^{p-23}, \quad p \neq 23; \quad \phi(x) \propto \ln r, \quad p = 23. \quad (6.5)$$

As discussed in Section 5, the open string tadpole in OCSFT is unchanged if we explicitly shift the closed string background to cancel the tadpole. This corresponds to turning on a linearized gravity background of the form (6.4). In OCSFT, the open string tadpole then arises by acting on this closed string background with the open-closed interaction vertex. Thus, in OCSFT, we can naturally think of the open string tadpole as coming directly from the closed string background arising from the D-brane.

In OSFT, the analysis in Section 3 of the small T expansion of the one-loop tadpole reveals a highly parallel structure to that just described. The terms in (3.31) associated with massless fields are those with a T dependence of the form $1/T^2$. The integration measure dT/T^2 is proportional to the measure ds for the dual (closed string) modular parameter. Unlike the closed string tadpole, the open string tadpole only has support at vanishing momentum $p = 0$. As discussed in Section 3, the integral over q_\perp in the closed string boundary state gives extra powers of T in the modular integral, so that when $p \leq 22$ the modular integral is convergent. This is analogous to smoothing out the solution (6.4) by integrating with the measure $\int d^{25-p}k_\perp \sim \int k_\perp^{24-p} dk_\perp$ in the vicinity of the singular point k_\perp . For $p \leq 22$ the resulting integral is convergent, while for $p \geq 23$ the integral diverges.

This somewhat schematic discussion indicates that part of the open string tadpole can be seen as arising from the closed string background associated with the Dp -brane. For $p \leq 22$, this piece of the tadpole is finite. In the following subsection, we consider D-branes for which this part of the tadpole diverges, and we develop the line of reasoning just described in more detail.

6.3 Divergent diagrams and BRST invariance

Having analyzed the case where the tadpole diagram is finite, we now turn to the cases where the diagram diverges². While we have no satisfactory way of regulating these diagrams, we

²We would like to thank Eva Silverstein for very useful discussions on the issues in this section and in Appendix A.1. A world-sheet discussion of issues related to the divergences we describe in this section will be given in [54]

can still extract some interesting physics from them. What we attempt to show is that BRST invariance mostly determines the physics hidden in the divergent part of the modular integral.

Recall from section 5 that, for the tadpole diagram, BRST invariance amounts to checking that Q_B annihilates the tadpole state, $|\mathcal{T}\rangle$. Since Q_B is a total derivative on moduli space, we will only pick up contributions at the boundaries of moduli space. In other words, we can only pick up surface terms at $T = 0$ and $T = \infty$. Such surface terms can, in fact, arise because of the divergences in the tadpole and are discussed in appendix A.

Since the $T \rightarrow 0$ limit of the tadpole diagram is divergent, we must introduce some sort of regulator. A very simple choice is to just cut off the modular integral at some minimum value T_0 . In other words, we replace $|\mathcal{T}\rangle$ with the regulated state

$$|\mathcal{T}\rangle_{T_0} = \int_{T_0}^{\infty} |\mathcal{T}(T)\rangle.$$

where we have included the subscript T_0 to explicitly indicate that this is a regulated form of the tadpole. Since the subscript T_0 is cumbersome, we drop it in subsequent equations, but, throughout this section, we will assume that $|\mathcal{T}\rangle$ is regulated in this way. Introducing the cutoff, T_0 , explicitly breaks the BRST invariance of the diagram. Acting on $|\mathcal{T}\rangle$ with Q_B gives a surface term at T_0 . This is seen in the following calculation

$$\begin{aligned} \langle \mathcal{T} | Q_B &= \int_{T_0}^{\infty} dT \langle V_3 | b_0^{(2)} e^{-TL_0} | \tilde{V}_2 \rangle Q_B \\ &= \int_{T_0}^{\infty} dT \frac{d}{dT} \langle V_3 | e^{-TL_0} | \tilde{V}_2 \rangle \\ &= \langle V_3 | e^{-T_0 L_0} | \tilde{V}_2 \rangle. \end{aligned} \tag{6.6}$$

Note that the last line of (6.6) is similar to the original tadpole diagram except that we have fixed the modular parameter at T_0 and dropped the insertion of b_0 . Thus in the conformal field theory method, we can represent the surface term by just taking $T \rightarrow T_0$ and dropping the integral of $b(z)$ across the world-sheet.

For the tadpole diagram to be BRST invariant, we would require that Q_B acting on the region of integration $T < T_0$ should cancel this surface term. Unfortunately, for the divergent diagrams, we can not define this region of integration. Thus we consider replacing the $T < T_0$ region of integration with a new diagram. We then try to understand what restrictions the condition of BRST invariance imposes. This condition will not fix the new diagram completely but will tell us something about the physics of the $T < T_0$ region.

To construct the new diagram, we start with the surface term we found from acting on $|\mathcal{T}\rangle$ with Q_B and modify it. As we discussed for the tadpole diagram, we may replace the boundary at the bottom of the surface term with a boundary state without changing the diagram. Instead of doing this, however, we replace the bottom of the diagram with some

arbitrary closed string field Φ . Call this new diagram $|\mathcal{T}_\Phi\rangle$. The surface term we found from acting on $|\mathcal{T}\rangle$ with Q_B can then be written as $|\mathcal{T}_B\rangle$.

We now propose replacing the region of integration $T < T_0$ with the surface term $|\mathcal{T}_\Phi\rangle$. To ensure that this choice of surface term is valid, one would have to show that any open string state can be written in the form $|\mathcal{T}_\Phi\rangle$ for some closed string state Φ . While, from the conformal field theory expression for $|\mathcal{T}_\Phi\rangle$, this seems likely, we will content ourselves with the fact that this choice of surface term is general enough for our purposes. With this caveat in mind, we can then ask: what condition does BRST invariance impose on Φ ? To check this we need to consider the action of Q_B on $|\mathcal{T}_\Phi\rangle$.

We now show that $Q_B|\mathcal{T}_\Phi\rangle = |\mathcal{T}_{(Q_B+\tilde{Q}_B)\Phi}\rangle$. This can be shown by a contour pulling argument. We start with the BRST current contour running across the external leg of the diagram and pull it to the right. Since the Witten vertex is BRST invariant, we can freely slide the contour over it. If we slide the two ends of the contour all the way to the right of the diagram, they eventually meet each other and we can join them together to form a closed contour. This contour can then be pulled down the tube at the bottom of the diagram to act on $|\Phi\rangle$. This process is pictured in figure 9.

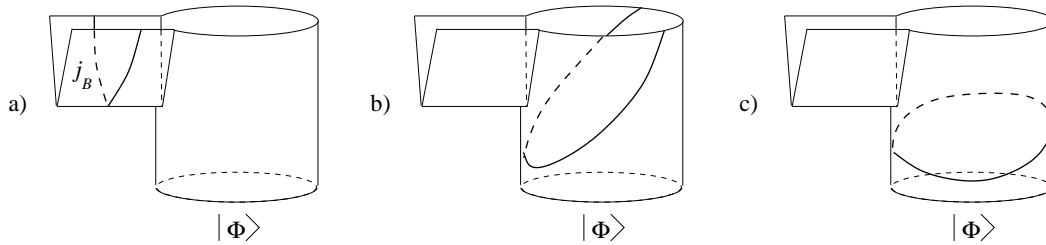


Figure 9: Contour pulling argument showing that $Q_B|\mathcal{T}_\Phi\rangle = |\mathcal{T}_{(Q_B+\tilde{Q}_B)\Phi}\rangle$. a) The contour of the BRST current j_B starts on the external leg. b) Pulling the contour to the right we can freely pass it over the Witten vertex. c) The two ends of the contour are joined together. The contour can now be thought of as acting on $|\Phi\rangle$.

Note that in the notation we are using we can write, $Q_B|\mathcal{T}\rangle = |\mathcal{T}_B\rangle$. Thus, if we modify the tadpole diagram by $|\mathcal{T}\rangle \rightarrow |\mathcal{T}\rangle + |\mathcal{T}_\Phi\rangle$, the condition for BRST invariance becomes

$$0 = Q_B(|\mathcal{T}\rangle + |\mathcal{T}_\Phi\rangle) = |\mathcal{T}_B\rangle + |\mathcal{T}_{(Q_B+\tilde{Q}_B)\Phi}\rangle = |\mathcal{T}_{B+(Q_B+\tilde{Q}_B)\Phi}\rangle. \quad (6.7)$$

So to cancel the BRST anomaly we should choose

$$(Q_B + \tilde{Q}_B)|\Phi\rangle = -|\mathcal{B}\rangle. \quad (6.8)$$

Notice that this is essentially the same closed string field we used when we shifted the OCSFT action.

We now try to solve for $|\Phi\rangle$. We restrict discussion to the D25-brane case since it is the simplest. Equation (6.8) was already solved in [26] and we follow the discussion there. First, note that equation (6.8) requires that the boundary state is BRST-closed and BRST-exact. While it is true that $(Q_B + \tilde{Q}_B)|\mathcal{B}\rangle = 0$, it is not true that $|\mathcal{B}\rangle$ is exact. This can be seen by

looking at the expansion of $|\mathcal{B}\rangle$ in equation (3.26). We can resolve this issue by noting that the cohomology of Q_B is defined using states with well-behaved momentum dependence. For example one can check that

$$Q_B x_0^\mu |0\rangle = c_1 \alpha_{-1}^\mu |0\rangle, \quad (6.9)$$

contrary to the fact that $c_1 \alpha_{-1}^\mu |0\rangle$ is in the cohomology of Q_B . Thus, we proceed by just taking a general state of weight $(0, 0)$ and $(-1, -1)$ fields, acting on it with $(Q_B + \tilde{Q}_B)$ and comparing it with $|\mathcal{B}\rangle$. We use the same parametrization for $|\Phi\rangle$ as [26]

$$|\Phi\rangle = \left(A(p) c_1 \tilde{c}_1 - \alpha_{-1}^\mu \tilde{\alpha}_{-1}^\nu h_{\mu\nu}(p) c_1 \tilde{c}_1 \right. \\ \left. + (c_1 c_{-1} - \tilde{c}_1 \tilde{c}_{-1}) (\Phi(p) - h_\mu^\mu(p)/2) + (c_0 + \tilde{c}_0) (c_1 \alpha_{-1}^\mu - \tilde{c}_1 \tilde{\alpha}_{-1}^\mu) i \zeta_\mu(p) \right) |0\rangle. \quad (6.10)$$

We then compute

$$(Q_B + \tilde{Q}_B) |\Phi\rangle = \left(\frac{1}{2} p^2 - 1 \right) A(p) c_1 (c_0 + \tilde{c}_0) \tilde{c}_1 |0\rangle \\ + \left[-\frac{1}{2} p^2 h_{\mu\nu}(p) + i p_\mu \zeta_\nu(p) + i p_\nu \zeta_\mu(p) \right] \alpha_{-1}^\mu \tilde{\alpha}_{-1}^\nu (c_0 + \tilde{c}_0) c_1 \tilde{c}_1 |0\rangle \\ + \left[\frac{1}{2} p^2 (\Phi(p) - h_\mu^\mu(p)/2) + i p^\mu \zeta_\mu(p) \right] (c_0 + \tilde{c}_0) (c_1 c_{-1} - \tilde{c}_1 \tilde{c}_{-1}) |0\rangle \\ + \left[-p^\mu h_{\mu\nu}(p) - p^\mu (\Phi(p) - h_\mu^\mu(p)/2) + 2i \zeta_\mu(p) \right] (\tilde{\alpha}_{-1} c_{-1} + \alpha_{-1} \tilde{c}_{-1}) c_1 \tilde{c}_1 |0\rangle. \quad (6.11)$$

Substituting equation (6.11) into $(Q_B + \tilde{Q}_B) |\Phi\rangle = -|\mathcal{B}\rangle$ gives

$$\left(\frac{1}{2} \partial^2 + 1 \right) A(x) = 1 \\ \frac{1}{2} \partial^2 h_{\mu\nu}(x) - \partial_\mu \zeta_\nu(x) - \partial_\nu \zeta_\mu(x) = \eta_{\mu\nu} \\ \frac{1}{2} \partial^2 \Phi(x) - \frac{1}{4} \partial^2 h_\mu^\mu(x) + \partial^\mu \zeta_\mu(x) = 1 \\ \frac{1}{2} \partial^\nu h_{\mu\nu}(x) + \frac{1}{2} \partial_\mu \Phi(x) - \frac{1}{4} \partial_\mu h_\nu^\nu(x) = \zeta_\mu(x). \quad (6.12)$$

If we eliminate $\zeta_\mu(x)$, these equations are equivalent to the linearized gravity equations in the background of the brane [26]. Note that the closed string tachyon shift is simply given by $A(p) = 1$.

To generalize to arbitrary p one must replace the R.H.S. of equation (6.12) with the appropriate source terms from the lower dimensional boundary states. These source terms will have δ -functions for the transverse dimensions. Solving these equations one can check that the long range behavior of the fields described in section 6.2 is reproduced.

Since the terms in $|\mathcal{B}\rangle$ of higher weight are BRST-exact we can act on them with

$$-\frac{b_0 + \tilde{b}_0}{L_0 + \tilde{L}_0} \quad (6.13)$$

to solve for the rest of $|\Phi\rangle$.

We have thus shown that BRST invariance of the tadpole implies that the region of integration $T < T_0$ should, for consistency, represent a closed string background. The fact

that this region of integration actually diverges, even when the solutions to the equations (6.12) are finite, arises from the specific prescription which OSFT uses to define the inverse of the BRST operator in terms of a closed string propagator.

One might ask why we cannot simply adopt this construction as a way of defining the tadpole. These are a number of problems with this idea. First, there is an ambiguity in the choice of Φ under the shift $\Phi \rightarrow \Phi + Q_B \delta \Phi$. This implies that if we were to use this scheme for one of the finite diagrams, we would, in general, get a different answer than the answer we would get from using analytic continuation. There is also the problem that we have introduced an unphysical parameter T_0 . One can check that this is not much of a problem since a shift in T_0 can be accommodated by a corresponding BRST exact shift of Φ . Perhaps the most serious problem with this somewhat arbitrary division of moduli space is that it would lead to a breakdown in unitarity since for $T < T_0$ one can no longer consider the tadpole to be made up of an open string loop.

Finding a sensible way of systematically dealing with the divergent massless closed string tadpoles encountered in this section seems to be an important problem for string field theory. Although these divergences are only associated with Dp -branes having codimension 3 or less, such branes are important to understand in string theory. While it seems difficult to make sense of the theory in, for example, a space-filling brane background, we know from the recent work on the Sen conjectures that string field theory in such a background contains within it other backgrounds corresponding to lower-dimensional D-branes and empty space-time. Since the theory is well defined in these other backgrounds, it seems that the technical problems encountered in the presence of high-dimensional D-branes should have some robust technical solution which does not require a significant modification of the theory. On the other hand, it may be possible that the theory does not have a well-defined perturbation series in all backgrounds. This question is particularly pressing for superstring field theory, where we might expect the theory to be completely well-defined with finite tadpoles for Dp -branes with $p < 7$, while Dp -branes with $p \geq 7$ would have similar divergences to those discussed in this section.

6.4 Beyond one loop

Having examined the divergences in the tadpole diagram we discuss the situation for higher-loop diagrams. Although we have no explicit computations, we predict that there will be additional divergences of a new kind. For example at the two-loop level one can consider a torus diagram with a hole. If we put an open string state on the edge of the hole we have a contribution to the two-loop tadpole diagram. In the conformal frame natural to OSFT this diagram is pictured in figure 10.

There is a region of moduli space in which the hole is separated from the rest of the diagram by a long tube. In this limit the diagram may be viewed as an open string which turns into a closed string which propagates over a long tube and then ends in a torus. This

long tube leads to a divergence and associated BRST anomaly in world-sheet string theory and represents a shift in the cosmological constant [26]. The divergence occurs both because of the closed string tachyon and the massless fields and thus cannot be treated by a simple analytic continuation.

We expect a similar divergence and BRST anomaly in OSFT. Just as the one-loop open string tadpole could be thought of as a coupling between the open strings and the closed string tadpole, here the two-loop open string tadpole can be thought of as a coupling between the open strings and the one-loop closed string tadpole. The closed string tadpole we studied in the context of the one-loop open string tadpole arose because the brane was a source for the closed string fields. The one-loop closed string tadpole occurs even in pure closed string theory in the absence of the brane. Thus we expect that the divergence we find will be independent of the number of transverse dimensions.

At higher loops still more diagrams with divergent long tubes appear. For every divergent closed string tadpole we will find a corresponding set of divergences in OSFT. Without some general framework, each of these divergences must be treated individually. To some extent, this same problem arises in ordinary world-sheet string theory, but one might have hoped that in OSFT the problem would be more tractable.

7. Discussion

In this paper we have explicitly calculated the one-loop open string field theory tadpole using both conformal field theory and oscillator methods and found that the calculations agree. There is a divergence in the loop diagram due to the propagation of an open string tachyon around the loop; this divergence is easily dealt with by analytic continuation in an expansion of the diagram in the level of the open string field in the loop using the oscillator approach to OSFT. We also find, however, that the one-loop tadpole diagram diverges due to the propagation of the closed string tachyon over a long closed string tube. This divergence arises only because we are working in bosonic string theory, and can also in principle be treated by analytic continuation. In practice, we can perform this analytic continuation for the one-loop diagram considered in this paper by explicitly using our knowledge of the role of closed strings in this diagram, but this is much more subtle than in the case of the open string tachyon, as the closed strings are not explicitly included as degrees of freedom in OSFT. The analytic continuation we use does not deal with the closed string tachyon

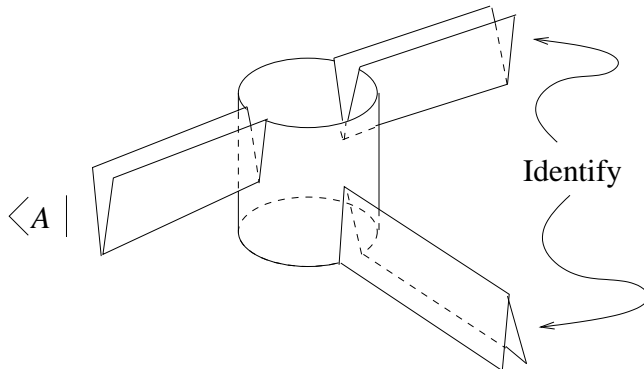


Figure 10: The two-loop non-planar tadpole diagram contributing to a breakdown in BRST invariance.

divergence successfully for low-codimension branes. This procedure is not easily generalized to more complicated diagrams, and we do not have any systematic way of dealing with such divergences other than order-by-order in perturbation theory.

Once we have treated the leading divergences in the one-loop tadpole by hand, the tadpole becomes finite as long as we work in a D-brane background with sufficiently many codimensions. For D-branes of dimension $p \geq 23$, we find divergences from the propagation of massless modes over long distances. For the D25-brane theory, this divergence also contributes to a BRST anomaly. It does not seem to be possible to treat these divergences without stepping outside the framework of OSFT. Indeed, recent work indicates that even the Fischler-Susskind mechanism for dealing with such divergences in the world-sheet formalism may have previously unexpected subtleties [53, 54]. We describe, however, a procedure for using BRST invariance that reveals much of the physics hidden in these divergent diagrams. Achieving a better understanding of these divergences seems to be an important unsolved problem for string field theory.

We have found that the open string tadpole essentially arises from the coupling between the closed string background and the open strings. The closed string has a tadpole in the presence of a D-brane, expressing the linearized massless fields produced by the D-brane source. The fact that this shift in the closed string background is seen in the one-loop tadpole diagram considered here demonstrates that OSFT actually captures the running of the background geometry, and thus contains a highly nontrivial aspect of closed string physics.

At two loops, OSFT runs into further difficulties with divergences and probably BRST anomalies as well. We believe that these problems, which are already well-known from perturbative string theory, doom any attempt to construct a complete quantum theory from bosonic open string field theory, without the introduction of some fundamental new idea. It is, of course, possible that some as-yet unknown mechanism stabilizes the closed string tachyon and turns bosonic string theory into a consistent theory. But if this is the case, this mechanism is no more apparent from the point of view of OSFT than from the traditional perturbative approach to the theory. In this sense, our study of quantum effects in bosonic OSFT has not led to any surprising new insights.

The positive results we have found here are, however, firstly that OSFT does not have any new problems or complications in the definition of the quantum theory which could not be predicted based on known issues in the perturbative theory, second that the one-loop tadpole in bosonic OSFT can be understood in a physically sensible fashion, and third that the OSFT tadpole naturally contains information about the shift in the closed string background due to the D-brane with respect to which the open string theory is originally defined.

While bosonic string theory has been a nice toy model with which to explore a variety of phenomena in string field theory, such as tachyon condensation, it remains unclear whether

this theory is connected in any fundamental way with supersymmetric string theory and M-theory, and even whether this theory can be defined in a complete and consistent fashion quantum mechanically. In order to make further progress in understanding how far string field theory can take us in probing the fundamental nature of string theory, when we begin to consider seriously the construction of a nonperturbative quantum theory, it is probably necessary to work with a supersymmetric string field theory. The results of this paper seem to give positive support to the hypothesis that supersymmetric open string field theory, if it exists classically, may naturally extend to a sensible quantum theory. Two possible candidates for SUSY OSFT are the Berkovits theory [55] and the Witten theory [56, 57, 58]. If one of these theories can be shown to be completely consistent and to correctly incorporate the Ramond as well as the NS sector of open strings, it seems likely that an analogous calculation to the one in this paper will, for Dp -branes with $p < 7$, give rise to a finite one-loop tadpole which encodes the linearized gravitational fields from the D-brane source. Such a tadpole should not suffer from any of the divergences encountered in this paper. In the supersymmetric theory, there seems to be no reason why higher loop calculations should not continue to incorporate the higher-order gravitational effects of the Dp -brane, so that the full theory should completely encode the Dp -brane geometry seen by closed strings.

There is clearly a significant amount of work remaining to be done to substantiate this story, but if this picture can be realized explicitly, it could open several exciting new directions for progress. This would give a new nonperturbative quantum definition of string theory. In this theory, if it is unitary, closed strings should arise as composite states. This would give a new more general open string model exhibiting open-closed string duality, from which the CFT description of strings in AdS space would arise as a special case in the usual decoupling limit. Because OSFT can be defined nonperturbatively, it is possible to imagine using level truncation to compute numerical approximations to finite nonperturbative quantities, thus potentially accessing new nonperturbative features of string theory. Because, as we have seen in this paper, the closed string background is encoded in the quantum open string diagrams, it is possible that changes in the closed string background might be studied completely in terms of OSFT, once a full definition of the quantum theory exists. At a more pragmatic level, if the methods of this paper are applied to SUSY OSFT, it should be possible to study directly the production of closed strings in dynamical open string tachyon condensation [59]. As was shown in recent work on this subject, a full physical understanding of the rolling tachyon requires treating the back reaction of the radiated closed strings on the rolling open string tachyon (see [60, 61] for a recent discussion and further references). String field theory seems like the natural context in which to study this process, and quantum computations in OSFT like the one in this paper may, even in the bosonic theory, shed light on this puzzle.

At a more technical level, we have seen in this paper that the two different approaches to computing OSFT diagrams, the oscillator approach and the CFT approach, give somewhat orthogonal information about the structure of the theory. The CFT approach has the ad-

vantage of giving analytic expressions for amplitudes. From these analytic expressions, it is possible to take the limit where open string modular parameters become small, which in some situations corresponds to the limit where closed string physics plays an important role. In this paper, as in [11], it was possible to analytically study the contribution from closed strings by expanding around this limit. On the other hand, the CFT approach is only tractable for simple diagrams. For any diagram at genus $g > 1$, the CFT approach is not easily applicable. Furthermore, even for computing finite diagrams at genus $g \leq 1$, the CFT approach gives a complicated integral expression in terms of implicitly defined functions, which can only be numerically approximated. The oscillator approach, unlike the CFT approach, can be applied to arbitrary diagrams of OSFT. It is even possible to imagine truncating OSFT at finite level and including a momentum cutoff so that even nonperturbative quantities in OSFT can be approximated by finite-dimensional integrals. While closed strings are not included exactly when OSFT is truncated at finite oscillator level, as we found in this paper the effects of closed strings can be clearly seen when the oscillator cutoff is sufficiently high; in the level-truncated theory, the closed strings act more like resonances than like asymptotic states. Although we found here that the closed string tachyon divergence made it difficult to extract other physical effects in the oscillator calculation, in a theory without closed string tachyons, like the superstring, it seems that the oscillator method should be a viable approach for approximating any loop diagram. Even for the bosonic theory, a general method for analytically continuing or otherwise taming the tachyon divergence—such as a Lorentzian world-sheet formulation—would allow us to extract useful physics from the oscillator method. Summarizing these observations, it seems likely that in further developments, such as in a systematic formulation of a quantum supersymmetric open string field theory, both these approaches to computations will play useful roles.

Acknowledgments

We would like to thank Erasmo Coletti, Bo Feng, Yang-Hui He, Hong Liu, Hiroshi Ooguri, Martin Schnabl, Ilya Sigalov, Eva Silverstein and Barton Zwiebach for useful discussions; we would like to thank Barton Zwiebach in particular for comments on the draft. Thanks to Eva Silverstein for sharing with us a preliminary version of [54]. The numerical computations in this work were done using *Mathematica*. This work was supported by the DOE through contract #DE-FC02-94ER40818.

A. The BRST anomaly in the D25-brane theory

We now study the BRST invariance of the tadpole in the D25-brane theory. In any BRST-quantized string theory, a basic condition for gauge invariance is that BRST-exact states decouple from on-shell diagrams. For the tadpole diagram, this condition is simply that Q_B should annihilate the tadpole.

In sections A.1 and A.2 we use conformal field theory and oscillator methods to compute the action of the BRST operator on the tadpole and find that the tadpole is not BRST closed. This breakdown of gauge invariance is familiar from ordinary string perturbation theory in the context of the Fischler-Susskind mechanism [28, 29, 30, 26, 52]. Our results differ from previous work on BRST invariance in OSFT. In [62] it was argued that $Q_B|\mathcal{T}\rangle$ should vanish, while in [8] it was suggested that it might be possible to avoid a breakdown in BRST invariance in Feynman-Siegel gauge. Our results indicate that in fact $Q_B|\mathcal{T}\rangle \neq 0$, even in Feynman-Siegel gauge.

A.1 The BRST anomaly in the conformal field theory method

We now study the BRST invariance of the OSFT tadpole for the D25-brane theory. On the grounds of gauge invariance, we expect that $Q_B|\mathcal{T}\rangle = 0$. To check this identity we first need to render $|\mathcal{T}\rangle$ a finite state by imposing a cutoff.

We choose to simply cut off the integrals over the modular parameter T so that it never gets smaller than some minimum value T_0 . We can then evaluate $Q_B|\mathcal{T}\rangle$ using equation (6.6). This gives

$$\langle \mathcal{T} | Q_B = \langle V_3 | e^{-T_0 L_0} | \tilde{V}_2 \rangle. \quad (\text{A.1})$$

We can then examine the behavior as $T_0 \rightarrow 0$. Conveniently, we have already done all the work for this calculation in section 3. Notice that the only difference between equation (A.1) and equation (4.2), is that T is evaluated at a specific point, T_0 , and that the b_0 is missing. In the conformal field theory language we can accommodate this change by simply fixing the length of the internal propagator to be T_0 and dropping the insertion of b_0 . This gives

$$Q_B|\mathcal{T}\rangle = U_{h(z)\circ z(v)}^\dagger \Big|_{T=T_0} (h(z) \circ z(w) \Big|_{T=T_0} \circ \mathcal{B})|0\rangle. \quad (\text{A.2})$$

To map the resulting diagram to the disk, we can just use the same map $z(w)$ given in equation (3.25). Since there is no b_0 to worry about, the divergence structure is actually much simpler. Since $U_{h(z)\circ z(v)}^\dagger$ is well behaved as $T_0 \rightarrow 0$ and $h(z)$ is independent of T_0 , we only need to consider $z(w) \circ \mathcal{B}$. Using equation (3.26) we get that the boundary state is mapped to

$$\begin{aligned} z \circ |\mathcal{B}\rangle &= \left(\frac{1 + W_0^2}{k_0 W_0^2} \right)^2 c_1 (c_0 + \tilde{c}_0) \tilde{c}_1 |0\rangle \\ &\quad - \alpha_{-1} \cdot \tilde{\alpha}_{-1} \tilde{c}_1 (c_0 + \tilde{c}_0) c_1 |0\rangle - 2(c_1 c_{-1} + \tilde{c}_{-1} \tilde{c}_1) (c_0 + \tilde{c}_0) |0\rangle \\ &\quad + \text{terms that vanish as } W_0 \rightarrow 0, \end{aligned} \quad (\text{A.3})$$

where W_0 is T_0/π and k_0 is $k(W_0)$. Clearly as $T_0 \rightarrow 0$ this expression is non-vanishing.

For theories on Dp branes with $p < 25$ we will still find an anomaly for the terms coming from the closed string tachyon but we no longer find an anomaly in the massless sector. For

example, the graviton/dilaton term in (A.3) in the Dp -brane theory becomes

$$\int d^{25-p}q_{\perp} \left(\frac{1+W_0^2}{k_0W_0^2} \right)^{q_{\perp}^2} \alpha_{-1} \cdot \tilde{\alpha}_{-1} \tilde{c}_1 (c_0 + \tilde{c}_0) c_1 |q_{\perp}\rangle. \quad (\text{A.4})$$

Mapping to the upper-half plane this becomes

$$\int d^{25-p}q_{\perp} (2)^{q_{\perp}} \left(\frac{1+W_0^2}{k_0W_0^2} \right)^{q_{\perp}^2} : c \partial X(i) \cdot \tilde{c} \bar{\partial} X(i) e^{iq_{\perp} \cdot X(i)} :. \quad (\text{A.5})$$

Now consider evaluating the correlation between this operator and the external state. When $e^{iq_{\perp} \cdot X(i)}$ contracts with itself we pick up a factor of $(2)^{-q_{\perp}}$. The operator $e^{iq_{\perp} \cdot X(i)}$ can also contract with other X 's but these just pick up factors of q_{\perp}^2 . Such terms will go to zero as $W \rightarrow 0$. Thus the largest contribution comes from the momentum integral

$$\int d^{25-p}q_{\perp} \left(\frac{1+W_0^2}{k_0W_0^2} \right)^{q_{\perp}^2} \propto \left[-\log \left(\frac{1+W_0^2}{k_0W_0^2} \right) \right]^{\frac{1}{2}(p-25)}, \quad (\text{A.6})$$

which vanishes as $W_0 \rightarrow 0$.

A.2 The BRST anomaly in level truncation

It is also possible to demonstrate the BRST anomaly in level truncation. It is easiest to frame this discussion in terms of truncation on field level rather than oscillator level. Let us begin by considering a level expansion of the regulated equation (6.6)

$$Q_B \int_{T_0}^{\infty} dT \langle \tilde{V}_2 | b_0 e^{-TL_0} | V_3 \rangle = \langle \tilde{V}_2 | e^{-T_0 L_0} | V_3 \rangle = \sum_n c_n(T_0) e^{(1-n)T_0}, \quad (\text{A.7})$$

where the term associated with the coefficient c_n arises from fields in the loop of level n . We can deal with the open string tachyon divergence through analytic continuation. The coefficients $c_n(T_0)$ are finite for all values of $n > 1, T_0 > 0$, and can be directly calculated by computing the contribution to either the first or the second expression in (A.7) at each level. Direct computation at low levels confirms that both ways of computing $c_n(T_0)$ give the same result. Truncating the theory at finite field level reduces the summation in (A.7) to a finite sum, from which we can take the $T_0 \rightarrow 0$ limit in the level-truncated theory. Thus, we see that (A.1) holds in level truncation, even as $T_0 \rightarrow 0$, so that level truncation naturally regulates the divergences in this equation arising from closed strings.

To show that (A.7) does not vanish in the limit $T_0 \rightarrow 0$, let us examine the action of Q_B on the level 2 sector of $|\mathcal{T}\rangle$. This calculation is straightforward, as Q_B conserves level. The fields appearing in $|\mathcal{T}\rangle$ at level 2 are

$$|\mathcal{T}^{(2)}\rangle = \left(\beta_{\mu\nu} a_1^{\dagger\mu} a_1^{\dagger\nu} + \gamma c_2^{\dagger} b_0 + \delta c_1^{\dagger} b_1^{\dagger} \right) c_0 |\hat{0}\rangle. \quad (\text{A.8})$$

Upon acting with Q_B we find

$$Q_B|\mathcal{T}^{(2)}\rangle = (\beta_\mu^\mu - \gamma - 3\delta) c_2^\dagger c_0 |\hat{0}\rangle. \quad (\text{A.9})$$

The condition that $|\mathcal{T}^{(2)}\rangle$ be Q_B -closed thus reduces to the condition

$$\beta_\mu^\mu - \gamma - 3\delta = 0 \quad (\text{A.10})$$

on the coefficients of the component states.

The coefficients $\beta_{\mu\nu}$, γ and δ are given by

$$\begin{aligned} \beta_{\mu\nu} &= \eta_{\mu\nu} \int_0^\infty dT S_0(T) \left(-\frac{1}{2} M_{11}(T)\right), \\ \gamma &= \int_0^\infty dT S_0(T) (-R_{20}(T)), \\ \delta &= \int_0^\infty dT S_0(T) (-R_{11}(T)). \end{aligned} \quad (\text{A.11})$$

As discussed above, level truncation serves to render the integrals in equation (A.11) finite, so that they are calculable numerically. The integrands become very sharply peaked near $T = 0$, so numerical analysis becomes difficult for small T . Nevertheless, it is clear that effects near $T = 0$ give rise to a violation of (A.10). At successively higher levels, the weight factor S_0 becomes more and more sharply peaked at $T = 0$, and the integral is well approximated by its endpoint value $-\frac{1}{2}M_{11}(0)S_0(0)$. As we have demonstrated above, $M_{11}(0) = R_{11}(0) = -1$, while $R_{20}(0) = 0$; these values manifestly fail to satisfy (A.10). Moreover, as we remove the regularization by sending the level to infinity, the violation becomes infinite.

We have thus seen in the operator formalism the presence of a breakdown in BRST invariance which can be directly ascribed to the presence of short-distance divergences, interpretable in terms of the closed string tachyon.

B. The infinite level limit

In this section we look at some of the subtleties of the infinite level limit of the matrices in the oscillator calculations. In particular, we are interested in comparing how level-truncated calculations near $T = 0$ compare with what we expect if we take the level to infinity.

For definiteness, we work in the ghost sector. The calculation in the matter sector is completely analogous. We begin by expanding the expression for R_{nm} , given in (4.21), around $T = 0$ in level truncation. The only tricky part of the calculation is the small T expansion of

$$\frac{1}{1 - S\tilde{X}}. \quad (\text{B.1})$$

It turns out, however, that it is sufficient to consider the expansion of (B.1) acting on $S \begin{pmatrix} X^{21} \\ X^{12} \end{pmatrix}$, which gives

$$\frac{1}{1 - S\tilde{X}} S \begin{pmatrix} X^{21} \\ X^{12} \end{pmatrix} = \begin{pmatrix} \mathbf{1} \\ \mathbf{1} \end{pmatrix} - T \left(\frac{1}{1 - S\tilde{X}} \Big|_{T=0} \right) \begin{pmatrix} \{G, CX^{21} + CX^{11}\} \\ \{G, CX^{12} + CX^{11}\} \end{pmatrix} + \mathcal{O}(T^2), \quad (\text{B.2})$$

where we have defined the matrix

$$G_{mn} = \frac{m}{2} \delta_{mn}. \quad (\text{B.3})$$

Using these formulas, one can work out the expansion

$$R_{mn} = C_{mn} - 2T\{G, C\}_{mn} + \mathcal{O}(T^2) = C_{mn} - 2mT C_{mn} + \mathcal{O}(T^2). \quad (\text{B.4})$$

In fact since the only identity needed to prove this relation is the sum rule $X^{11} + X^{12} + X^{21} = C$, equation(B.4) holds exactly at every fixed level.

We now make the following claim: In spite of the fact that the leading order correction is the same at every finite level, if we did not truncate the matrices at all, we would get instead

$$R_{mn} = C_{mn} - mT C_{mn} + \mathcal{O}(T^2). \quad (\text{B.5})$$

To see how this happens, consider a single matrix element R_{11} . We expect from level-truncated analysis that $R_{11}(T) = -1 + 2T + \mathcal{O}(T^2)$. In figure 11, we plot $-\frac{d}{dT}R_{11}(T)$ near zero at various levels. We see that if we go extremely close to zero, $-\frac{d}{dT}R_{11}(T)$ always eventually approaches -2 as predicted by (B.4).

As the level is increased, however, the region where $-\frac{d}{dT}R_{11}(T)$ is close to -2 becomes arbitrarily small. This falloff near $T = 0$ is analogous to the falloff we found when studying the tachyon divergence in section 4.2. If we imagine taking the level to infinity and then taking $T \rightarrow 0$, we can ignore the falloff region and just take

$$\lim_{T \rightarrow 0} \left(-\frac{d}{dT}R_{11}(T) \right) = -1, \quad (\text{B.6})$$

as predicted by the conformal field theory method.

We can now ask: what went wrong with the calculation of equation (B.4)? To analyze this question, it is convenient to work with the matrices $M^{ij} = CX^{ij}$. In level truncation these matrices satisfy one identity

$$M^{11} + M^{12} + M^{21} = 1. \quad (\text{B.7})$$

If we do not truncate the matrices, they also satisfy [63]

$$(M^{11})^2 + (M^{12})^2 + (M^{21})^2 = 1, \quad (\text{B.8})$$

and commute. These identities imply that at $T = 0$, the matrix $1 - S\tilde{X}$ has a non-vanishing kernel. Thus the matrix

$$\frac{1}{1 - S\tilde{X}} \Big|_{T=0} \quad (\text{B.9})$$

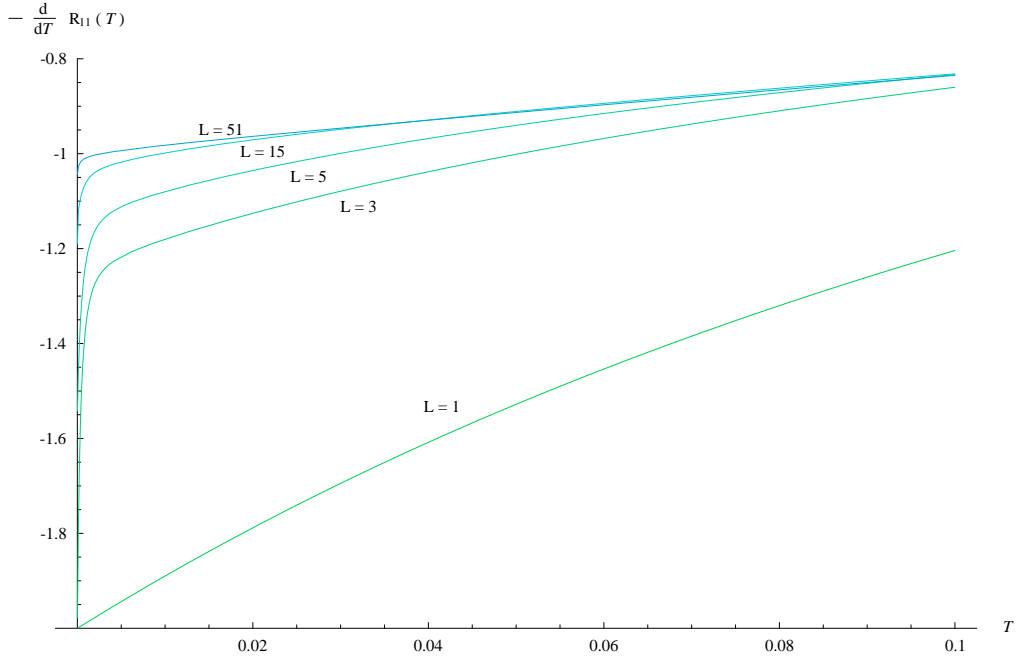


Figure 11: Plot of $-\frac{d}{dT} R_{11}(T)$ at various levels, L . We see that near $T = 0$, $-\frac{d}{dT} R_{11}(T)$ always approaches -2 , but at high levels comes arbitrarily close to hitting -1 .

is ill-defined. This invalidates the expansion (B.2). Even worse, the expression (4.28) that we used to see that $R_{nm} \rightarrow C$ as $T \rightarrow 0$ is not defined for the untruncated matrices. In fact one can check that while it is true that

$$\lim_{\text{Level} \rightarrow \infty} \left\{ \lim_{T \rightarrow 0} \left(\hat{X}^{12} \hat{X}^{21} \right) \frac{1}{1 - S\tilde{X}} \right\} = (C \ C), \quad (\text{B.10})$$

one finds that

$$\lim_{T \rightarrow 0} \left\{ \lim_{\text{Level} \rightarrow \infty} \left(\hat{X}^{12} \hat{X}^{21} \right) \frac{1}{1 - S\tilde{X}} \right\} \neq (C \ C) \quad (\text{B.11})$$

in a similar manner to what we found for $-\frac{d}{dT} R_{11}(T)$.

In spite of this, we find that $R_{nm} \rightarrow C$ in the small T limit unambiguously in numerical tests. At this time, we do not have enough control over the matrices \tilde{M} and \tilde{X} to give an infinite level proof of the identity B.5.

References

- [1] E. Witten, “Noncommutative Geometry And String Field Theory,” Nucl. Phys. B **268**, 253 (1986).
- [2] A. Sen, “Universality of the tachyon potential,” JHEP **9912**, 027 (1999) [hep-th/9911116](#).
- [3] K. Ohmori, “A review on tachyon condensation in open string field theories,” [hep-th/0102085](#).

- [4] P. J. De Smet, “Tachyon condensation: Calculations in string field theory,” [hep-th/0109182](#).
- [5] B. Zwiebach, “Is The String Field Big Enough?,” *Fortsch. Phys.* **49**, 387 (2001).
- [6] W. Taylor, “Lectures on D-branes, tachyon condensation, and string field theory,” [hep-th/0301094](#).
- [7] T. Asakawa, T. Kugo and T. Takahashi, “One-loop tachyon amplitude in unoriented open-closed string field theory,” *Prog. Theor. Phys.* **102**, 427 (1999) [hep-th/9905043](#); M. Alishahiha, “One-loop correction of the tachyon action in boundary superstring field theory,” *Phys. Lett. B* **510**, 285 (2001) [hep-th/0104164](#); K. Bardakci and A. Konechny, “Tachyon condensation in boundary string field theory at one loop,” [hep-th/0105098](#); B. Craps, P. Kraus and F. Larsen, “Loop corrected tachyon condensation,” *JHEP* **0106**, 062 (2001) [hep-th/0105227](#); G. Arutyunov, A. Pankiewicz and B. . Stefanski, “Boundary superstring field theory annulus partition function in the presence of tachyons,” *JHEP* **0106**, 049 (2001) [hep-th/0105238](#); J. A. Minahan, “Quantum corrections in p-adic string theory,” [hep-th/0105312](#); T. Lee, K. S. Viswanathan and Y. Yang, “Boundary string field theory at one-loop,” *J. Korean Phys. Soc.* **42**, 34 (2003) [hep-th/0109032](#); O. Andreev and T. Ott, “On one-loop approximation to tachyon potentials,” *Nucl. Phys. B* **627**, 330 (2002) [hep-th/0109187](#).
- [8] C. B. Thorn, “String Field Theory,” *Phys. Rept.* **175**, 1 (1989).
- [9] D. J. Gross, A. Neveu, J. Scherk and J. H. Schwarz, “Renormalization and unitarity in the dual resonance model,” *Phys. Rev.* **D2** (1970) 697.
- [10] C. Lovelace, “Pomeron form factors and dual Regge cuts,” *Phys. Lett.* **B34** (1971) 500.
- [11] D. Z. Freedman, S. B. Giddings, J. A. Shapiro and C. B. Thorn, “The Nonplanar One Loop Amplitude In Witten’s String Field Theory,” *Nucl. Phys. B* **298**, 253 (1988).
- [12] J. A. Shapiro and C. B. Thorn, “BRST-Invariant Transitions Between Closed And Open Strings,” *Phys. Rev. D* **36**, 432 (1987).
- [13] J. A. Shapiro and C. B. Thorn, “Closed String - Open String Transitions And Witten’s String Field Theory,” *Phys. Lett. B* **194**, 43 (1987).
- [14] B. Zwiebach, “Interpolating string field theories,” *Mod. Phys. Lett. A* **7**, 1079 (1992) [hep-th/9202015](#).
- [15] A. Hashimoto and N. Itzhaki, “Observables of string field theory,” *JHEP* **0201**, 028 (2002) [hep-th/0111092](#).
- [16] D. Gaiotto, L. Rastelli, A. Sen and B. Zwiebach, “Ghost structure and closed strings in vacuum string field theory,” [hep-th/0111129](#).
- [17] M. Alishahiha and M. R. Garousi, “Gauge invariant operators and closed string scattering in open string field theory,” *Phys. Lett. B* **536**, 129 (2002), [hep-th/0201249](#); M. R. Garousi and G. R. Maktabdaran, “Excited D-brane decay in cubic string field theory and in bosonic string theory,” *Nucl. Phys. B* **651**, 26 (2003) [hep-th/0210139](#).

- [18] A. Strominger, “Closed strings in open string field theory,” *Phys. Rev. Lett.* **58** 629 (1987); M. Srednicki and R. Woodard, “Closed from open strings in Witten’s theory,” *Nucl. Phys.* **B293**, 612 (1987), [hep-th/0201249](#); J. A. Harvey, P. Kraus, F. Larsen and E. J. Martinec, “D-branes and strings as non-commutative solitons,” *JHEP* **0007**, 042 (2000); [hep-th/0005031](#) G. W. Gibbons, K. Hori and P. Yi, “String fluid from unstable D-branes,” *Nucl. Phys. B* **596**, 136 (2001) [hep-th/0009061](#); A. Sen, “Fundamental strings in open string theory at the tachyonic vacuum,” *J. Math. Phys.* **42**, 2844 (2001) [hep-th/0010240](#); A. A. Gerasimov and S. L. Shatashvili, “Stringy Higgs mechanism and the fate of open strings,” *JHEP* **0101**, 019 (2001), [hep-th/0011009](#); G. Chalmers, “Open string decoupling and tachyon condensation,” *JHEP* **0106**, 012 (2001) [hep-th/0103056](#); S. L. Shatashvili, “On field theory of open strings, tachyon condensation and closed strings,” [hep-th/0105076](#); G. Moore and W. Taylor, “The singular geometry of the sliver,” *JHEP* **0201**, 004 (2002) [hep-th/0111069](#); D. Gaiotto, N. Itzhaki and L. Rastelli, “Closed strings as imaginary D-branes,” [hep-th/0304192](#).
- [19] J. M. Maldacena, “The large N limit of superconformal field theories and supergravity,” *Adv. Theor. Math. Phys.* **2**, 231 (1998) [*Int. J. Theor. Phys.* **38**, 1113 (1999)] [hep-th/9711200](#).
- [20] O. Aharony, S. S. Gubser, J. M. Maldacena, H. Ooguri and Y. Oz, “Large N field theories, string theory and gravity,” *Phys. Rept.* **323**, 183 (2000) [hep-th/9905111](#).
- [21] E. D’Hoker and D. Z. Freedman, “Supersymmetric gauge theories and the AdS/CFT correspondence,” [hep-th/0201253](#).
- [22] S. Giddings, “The Veneziano amplitude from interacting string field theory,” *Nucl. Phys.* **B278** 242 (1986).
- [23] J. H. Sloan, “ The scattering amplitude for four off-shell tachyons from functional integrals,” *Nucl. Phys.* **B302** 349 (1988).
- [24] S. Samuel, “Covariant off-shell string amplitudes,” *Nucl. Phys.* **B308** 285 (1988).
- [25] W. Taylor, “Perturbative diagrams in string field theory,” [hep-th/0207132](#).
- [26] J. Polchinski, “Factorization Of Bosonic String Amplitudes,” *Nucl. Phys. B* **307**, 61 (1988).
- [27] P. Di Vecchia, M. Frau, I. Pesando, S. Sciuto, A. Lerda and R. Russo, “Classical p-branes from boundary state,” *Nucl. Phys. B* **507**, 259 (1997) [hep-th/9707068](#).
- [28] W. Fischler and L. Susskind, “Dilaton Tadpoles, String Condensates And Scale Invariance,” *Phys. Lett. B* **171**, 383 (1986).
- [29] S. R. Das and S. J. Rey, “Dilaton Condensates And Loop Effects In Open And Closed Bosonic Strings,” *Phys. Lett. B* **186**, 328 (1987).
- [30] W. Fischler, I. R. Klebanov and L. Susskind, “String Loop Divergences And Effective Lagrangians,” *Nucl. Phys. B* **306**, 271 (1988).
- [31] I. Bars, I. Kishimoto and Y. Matsuo, “String amplitudes from Moyal string field theory,” [hep-th/0211131](#).

- [32] A. Leclair, M. E. Peskin and C. R. Preitschopf, “String field theory on the conformal plane (I)” *Nucl. Phys.* **B317** (1989) 411-463.
- [33] M. R. Gaberdiel and B. Zwiebach, “Tensor constructions of open string theories 1., 2.,” *Nucl. Phys.* **B505** (1997) 569, [hep-th/9705038](#); *Phys. Lett.* **B410** (1997) 151, [hep-th/9707051](#).
- [34] D. J. Gross and A. Jevicki, “Operator Formulation Of Interacting String Field Theory,” *Nucl. Phys. B* **283**, 1 (1987).
- [35] D. J. Gross and A. Jevicki, “Operator Formulation Of Interacting String Field Theory. 2,” *Nucl. Phys. B* **287**, 225 (1987).
- [36] E. Cremmer, A. Schwimmer and C. Thorn, “The vertex function in Witten’s formulation of string field theory” *Phys. Lett.* **B179** 57 (1986).
- [37] S. Samuel, “The physical and ghost vertices in Witten’s string field theory,” *Phys. Lett.* **B181** 255 (1986).
- [38] N. Ohta, “Covariant interacting string field theory in the Fock space representation,” *Phys. Rev.* **D34** (1986), 3785; *Phys. Rev.* **D35** (1987), 2627 (E).
- [39] L. Rastelli, A. Sen, and B. Zwiebach, “Classical Solutions in String Field Theory Around the Tachyon Vacuum”, *Adv. Theor. Math. Phys.* 5:393-428 (2002) [hep-th/0102112](#).
- [40] S. B. Giddings and E. J. Martinec, “Conformal Geometry And String Field Theory,” *Nucl. Phys. B* **278**, 91 (1986).
- [41] S. B. Giddings, E. J. Martinec and E. Witten, “Modular Invariance In String Field Theory,” *Phys. Lett. B* **176**, 362 (1986).
- [42] B. Zwiebach, “A Proof That Witten’s Open String Theory Gives A Single Cover Of Moduli Space,” *Commun. Math. Phys.* **142**, 193 (1991).
- [43] G. Zemba and B. Zwiebach, “Tadpole Graph In Covariant Closed String Field Theory,” *J. Math. Phys.* **30**, 2388 (1989).
- [44] A. LeClair, M. E. Peskin and C. R. Preitschopf, “String Field Theory On The Conformal Plane. 2. Generalized Gluing,” *Nucl. Phys. B* **317**, 464 (1989).
- [45] L. Rastelli and B. Zwiebach, “Tachyon potentials, star products and universality,” *JHEP* **0109**, 038 (2001) [hep-th/0006240](#).
- [46] M. Schnabl, “Wedge states in string field theory,” *JHEP* **0301**, 004 (2003) [hep-th/0201095](#).
- [47] M. Schnabl, “Anomalous reparametrizations and butterfly states in string field theory,” *Nucl. Phys. B* **649**, 101 (2003) [hep-th/0202139](#).
- [48] W. Taylor, “D-brane effective field theory from string field theory”, *Nucl. Phys.* B585:171-192 (2000) [hep-th/0001201](#).

- [49] V. A. Kostelecký and R. Potting, “Analytical construction of a nonperturbative vacuum for the open bosonic string”, Phys. Rev. D63:046007 (2001) [hep-th/0008252](#).
- [50] B. Zwiebach, “Oriented open-closed string theory revisited,” Annals Phys. **267**, 193 (1998) [hep-th/9705241](#).
- [51] B. Zwiebach, “Quantum Open String Theory With Manifest Closed String Factorization,” Phys. Lett. B **256**, 22 (1991).
- [52] M. B. Green, “The Influence Of World Sheet Boundaries On Critical Closed String Theory,” Phys. Lett. B **302**, 29 (1993) [hep-th/9212085](#).
- [53] A. Adams, J. McGreevy and E. Silverstein, “Decapitating tadpoles,” [hep-th/0209226](#).
- [54] J. McGreevy and E. Silverstein, *to appear*.
- [55] N. Berkovits, “SuperPoincare invariant superstring field theory,” Nucl. Phys. B **450**, 90 (1995) [Erratum-ibid. B **459**, 439 (1996)] [hep-th/9503099](#).
- [56] E. Witten, “Interacting Field Theory Of Open Superstrings,” Nucl. Phys. B **276**, 291 (1986).
- [57] C. R. Preitschopf, C. B. Thorn and S. A. Yost, “Superstring Field Theory,” UFIFT-HEP-90-3 *Invited talk given at Workshop on Superstring and Particle Theory, Tuscaloosa, AL, Nov 8-11, 1989*
- [58] I. Y. Arefeva, P. B. Medvedev and A. P. Zubarev, Phys. Lett. B **240**, 356 (1990).
- [59] A. Sen, “Rolling tachyon,” JHEP **0204**, 048 (2002) [hep-th/0203211](#); A. Sen, “Tachyon matter,” JHEP **0207**, 065 (2002) [hep-th/0203265](#).
- [60] F. Leblond and A. W. Peet, “SD-brane gravity fields and rolling tachyons,” [hep-th/0303035](#).
- [61] N. Lambert, H. Liu and J. Maldacena, “Closed strings from decaying D-branes,” [hep-th/0303139](#).
- [62] A. R. Bogojevic, “BRST Invariance Of The Measure In String Field Theory,” Phys. Lett. B **198**, 479 (1987).
- [63] L. Rastelli, A. Sen, and B. Zwiebach, “Star Algebra Spectroscopy”, JHEP 0203:029 (2002) [hep-th/0111281](#).